Eindhoven University of Technology
Faculty of Architecture, Building and Management
Department of Structural Design

Report TUE-BCO-01-19

Joint properties of plybamboo sheets in prefabricated housing

Guillermo González

Supervisors:

Prof. Frans van Herwijnen
Prof. Dr. Jorge Gutiérrez
Dr. Jules Janssen
Dr. Faas Moonen

September 2001

TABLE OF CONTENTS

ACKNOWLEDGEMENTS

This report would have not been possible to carried out without the unconditional help of Dr. Jules Janssen and Dr. Faas Moonen who were there week after week trying to understand the strange things that I came up with and giving ideas for the improvement of the research.
Of equal importance was the help of my promoters prof. Frans van Herwijnen and prof. Dr. Jorge Gutiérrez who were always trying to improve the quality of the work.
Special thanks to Martien Ceelen, Theo van de Loo and Rien Canters for all the help given in order to make the experimental tests possible and successful. In general, I would like to thank all the people in the laboratory to contribute in anyway on this research.
Finally, I would like to thank my dad and my sisters for the continuous support regardless of the distance and my future wife Catalina who is always a motivation to continue with the whole research.

NOTATION

The following notation is defined for each chapter. Other notation is defined in the appendices.

Chapter 1:

MB: bamboo mat boards from India, 12 mm thick [1].

SB: bamboo strip boards from China, 18 mm thick (Qinfeng Bamboo Flooring).

Chapter 2:

C: seismic coefficient.

k: rigidity in N/mm or N/mm^2.

w: uniform distributed load per area in N/mm^2 or kN/m^2.

L: length in mm.

b: width in mm.

E: modulus of elasticity in N/mm^2.

I: moment of inertia or second moment of area in mm^4.

EI: modulus of rigidity in Nmm^2.

ν : Poisson's coefficient.

m_y: elastic moment in Nmm or Nmm/mm.

σ_y : bending yield stress in N/mm^2.

t: thickness in mm.

p: uniform distributed load per length in N/mm or kN/m.

A: area in mm^2.

h: height in mm.

$F_{T,B}$: force transmitted by the top and bottom connection between the vertical members and the soleplates or horizontal members in N or kN.

R: capacity to resist lateral load or shear load in N or kN.

S_1: nail spacing for connection between plybamboo sheet and upper or lower soleplate or horizontal member in mm.

S_3: nail spacing for connection between plybamboo sheet and vertical members in mm.

x: horizontal axis of coordinates system.

y: vertical axis of coordinates system.

$F_{x,i}$: horizontal force for fastener i in N or kN.

$F_{y,i}$: vertical force for fastener i in N or kN.

x_i : x position for fastener i according to the x-y coordinates system in mm.

y_i : y position for fastener i according to the x-y coordinates system in mm.

F_i : force in fastener i in N or kN.

M : external moment in Nmm or kNm.

F_{max} : horizontal force for fastener i in N or kN.

x_{max} : maximum x position for fastener i in mm.

Chapter 3

b': experimental model width for corner and T-connections in mm.

l: experimental model length for corner and T-connections in mm.

F: load applied to the experimental models in N or kN.

d: distance between two points in mm.

B1: horizontal joint between horizontal sheet and 75x50 mm wood piece.

B2: vertical joint between 75x50 mm and 75x75 mm wood pieces.

B3: horizontal joint between 75x75 mm and 75x50 mm wood pieces.

B4: vertical joint between 75x50 mm wood piece and vertical sheet.

θ : angle of rotation in degrees.

F_y, F_u, θ_y, $\delta_{o,y}$, F_{LC} and F_{CM}: defined in page 25.

δ : displacement in mm.

r_i : initial rigidity in N/mm or kN/m.

A_x: horizontal reaction in support A which is detail 1 in Figure 3-4.

A_y: vertical reaction at support *A*.

C_x: horizontal reaction at support *C* which is detail 2 in Figure 3-4.

C_y: vertical reaction at support *C*.

M_{B1}: moment at B1.

M_{B2}: moment at B2.

M_{B3}: moment at B3.

M_{B4}: moment at B4.

B_{1x}: horizontal reaction at B1.

B_{1y}: vertical reaction at B1.

B_{2x}: horizontal reaction at B2.

B_{2y}: vertical reaction at B2.

B_{3x}: horizontal reaction at B3.

B_{3y}: vertical reaction at B3.

B_{4x}: horizontal reaction at B4.

B_{4y}: vertical reaction at B4.

x_1, x_2, y_1, y_2 : see Figure 3-15.

Chapter 4

T1, T2, T3: T-connection 1, 2 and 3 respectively (see Figure B-1).

$2F_y$, $2F_u$, $\delta_{o,y}$, $\delta_{1,y}$, $\delta_{2,y}$: defined in page 40.

$\sum M_1$: sum of moments at point 1 (see Figure 4-12).

$2F_1$: reaction force at the bottom support of the experimental T-connection in N or kN (see Figure 4-11).

F_2 : reaction forces at the horizontal supports of the experimental T-connection in N or kN (see Figure 4-11).

A, B, C, a, b, c, d : defined in Figure 4-11.

P_{cr}: buckling critical load in N or kN.

L_{ef}: effective length in mm.

E_c: compression modulus of elasticity in N/mm^2.

Chapter 5

M_1: external moment caused by lateral load applied to one panel in Nmm or kNm.

M_2: external moment caused by lateral load applied to the experimental model in Nmm or kNm.

R_1: lateral load applied to one panel in N or kN.

R_2: lateral load applied to the experimental model in N or kN.

T : tension force in N or kN.

C : compression force in N or kN.

F_y, δ_y, δ_u : defined in Figure 5-7.

t_1, t_2, $f_{h,1}$: defined in appendix D.

T_1, T_2, T_3 : tension forces in vertical member in N or kN (see Figure 5-13).

All dimensions are given in mm.

1 INTRODUCTION

This report deals with the theoretical and experimental structural analysis of the house design method using plybamboo sheets proposed by the author and his supervisors in the article '*Selection criteria for a house design method using plybamboo sheets*' [8]. The work concentrates on wall to wall connections such as corners, T and sheet to frame connection under lateral load. For the experimental tests, scale models were built and tested in order to obtain information about the structural behavior and capacity of such connections. With this knowledge, full-scale models would be built and tested with the purpose of guaranteeing the applicability of the design method concerning structural adequacy.

This report is divided in four chapters and five appendices.

The following chapter introduces the design method into a structural analysis which explains how the seismic and wind forces are transmitted in the house. This analysis facilitates the design of experiments for joints (the core of the report) and structural elements including its connections (further research). The chapter is complemented by appendices B, C and F. The first one presents an example of a hypothetic house showing the floor plan, fabrication plan of panel walls, connections between walls, wall to foundation and wall to roof. The second one is about the calculation of wind and seismic forces in hypothetic conditions using the International Building Code 2000 [6]. Appendix F shows the calculation of several design values according to Eurocode 5 [7].

Chapter 3 deals with the experimental tests for corner connections. These tests helped to improve the original design of such connection. Appendix D complements the chapter with theoretical capacities of nailed and screwed joints between wooden and plybamboo members calculated according to Eurocode 5 [7].

Chapter 4 is about experimental tests for T-connections. These tests corroborated that this connection is one of the strongest link in the structural chain.

Finally, chapter 5 concludes the report with experimental tests for sheet to frame connections under lateral load. Appendix E shows all the results obtained from these tests.

Appendix A gives some mechanical, physical and geometrical properties of the bamboo mat boards (MB) and strip boards (SB) that were used in the experimental tests.

2 STRUCTURAL ANALYSIS

2.1 Introduction

This chapter concentrates on the structural analysis of the house design method that has been proposed for building with plybamboo sheets (see appendix B).
Figure 2-1 shows which structural elements are considered in the analysis when the house is submitted to wind or seismic load. The roof and the roof structure are not considered in the analysis because the research is focused on walls.

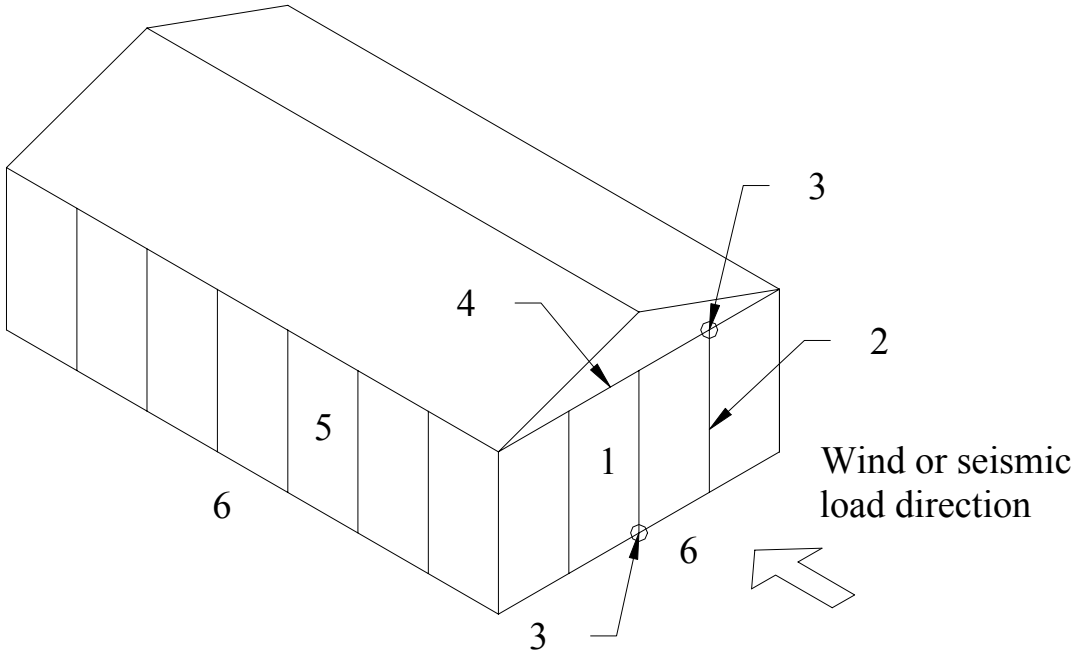

Figure 2-1 Structural components in the house design method.

Structural elements according to Figure 2-1:

1. Sheets in bending perpendicular to the plane (section 2.2).
2. Vertical members in bending (section 2.3).
3. Top or bottom connections (section 2.4)
4. Upper soleplate and its connections (section 2.5).
5. Shear walls (section 2.6).
6. Foundation

In section 2.7 the possible suction effect on the sheet is considered. Finally, conclusions are given in section 2.8.

2.2 Sheets in bending

The sheets will receive the wind or earthquake loads perpendicular to their plane (see Figure C-1 in appendix C). The wind load will be in this case higher than the earthquake effect because the equivalent seismic load will be only the weight of the panel multiplied by the seismic coefficient *C* (see appendix C, section C.2).
Each sheet can be modeled as a plate supported along its four sides as shown in Figure 2-2.

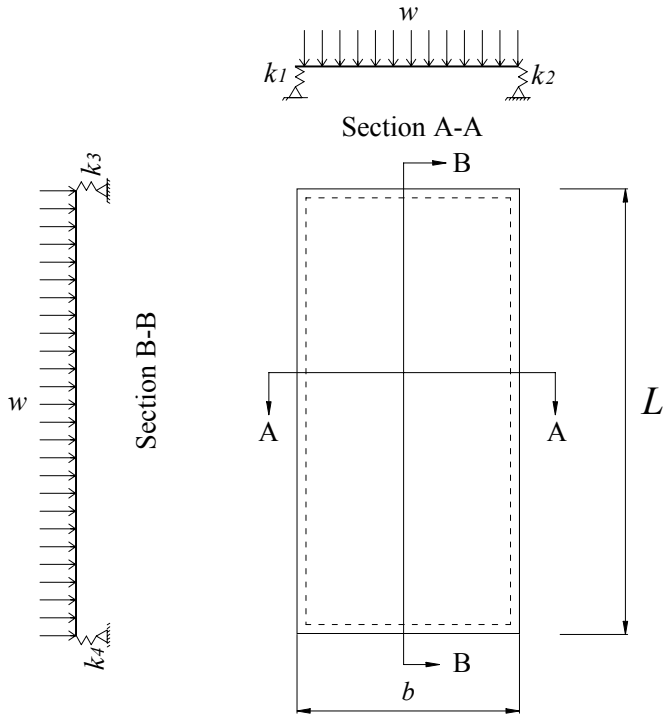

Figure 2-2 Plybamboo sheet submitted to load perpendicular to its plane.

The rigidities k_i will depend upon the modulus of rigidity (E_iI_i) of each of the corresponding horizontal or vertical members. In general all members will have the same modulus of rigidity except the lower soleplate which would be directly anchored to the foundation and can be considered as a simple support (hinge). The vertical elements that are connected to lateral walls could also be considered as simple supports. In order to simplify the calculations, all edges will be considered as simply supported. This consideration could not be seen as conservative since stress concentrations could occur in zones near the strongest supports. However, it gives an idea of the stress magnitudes that could be expected in the sheet.
From theory of plates, the elastic moment in the center of the sheet of Figure 2-2 when L/b = 2, $\nu = 0.3$ and $k_1 = k_2 = k_3 = k_4 = \infty$ is given by [3]:

$$m_y = 0.1017 w b^2 \qquad \textbf{(2-1)}$$

It is known from beam theory that:

$$m_y = \sigma_y t^2 / 6 \qquad \textbf{(2-2)}$$

Where, σ_y is the maximum yield stress in the sheet and t is the sheet thickness.

Taking the values $\sigma_y = f_{m,d} = 36$ N/mm^2 (design bending strength), $t = 12$ mm and $b = 1250$ mm (see Table A-1 in appendix A) and combining equations (2-1) and (2-2) a value of $w = 5.4$ kN/m^2 can be found. This value is 4.9 times higher than the wind load (1.1 kN/m^2) according to IBC 2000 [6] calculated in section C.1.

2.3 Vertical members

The vertical members (see section B-2) of the wooden frames are considered as simply supported beams with uniform distributed load p (see Figure 2-3a).

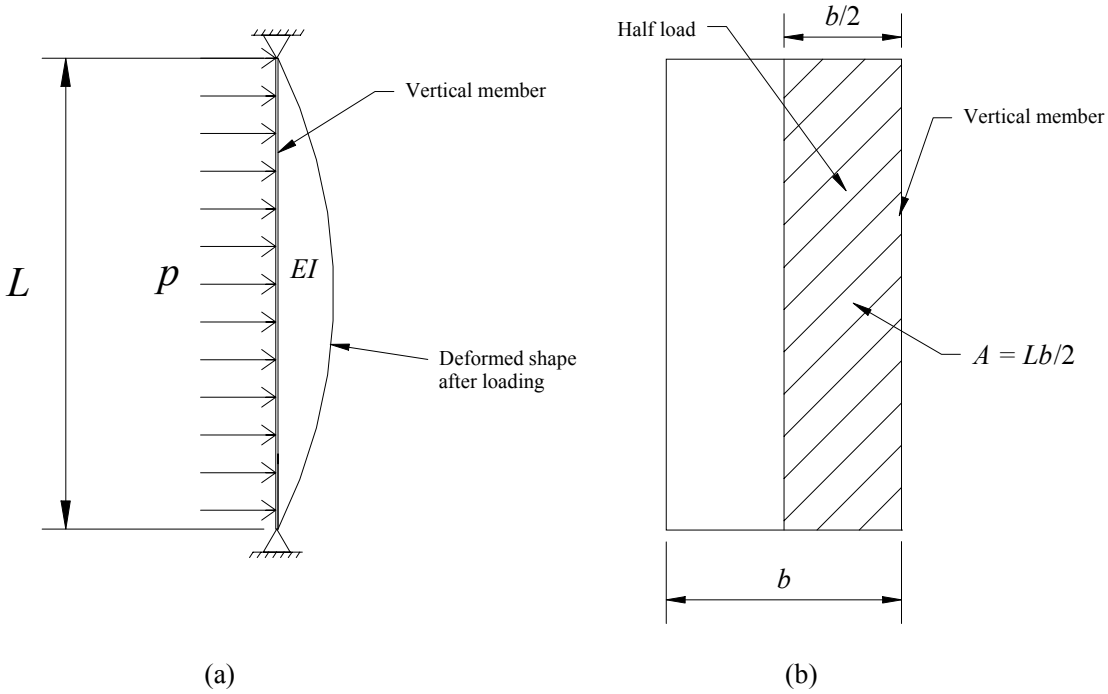

Figure 2-3 (a) Simply supported beam with uniform distributed load. (b) Vertical member taking half of the load received by the sheet.

From beam theory, the maximum moment in the beam is:

$$m_y = 0.125\,pL^2 = h^2 b\sigma_y / 6 \qquad \textbf{(2-3)}$$

Taking the values $L = 2500$ mm, $\sigma_y = f_{m,d} = 20$ N/mm^2 (design bending stress for wood class K24), $b = 50$ mm (beam width) and $h = 75$ mm (beam height), a value of $p = 1.2$ kN/m is found. This value can be transformed to a load per area $w = 1.2/0.625 = 1.9$ kN/m^2 where $0.625 = b/2$ ($b = 1250$ mm). This capacity is 1.7 times higher than the wind load according to IBC 2000 (see section C.1).

2.4 Top and bottom connections

The top and bottom connections will transmit the reaction forces $F_{T,B}$ to the upper and lower soleplates in case that panel C (Figure B-2 in appendix B) is used and to the upper and lower horizontal members in case that panels A and B (Figure B-2 in appendix B) are used. Figure 2-4 shows a proper way of making these connections. It consists of an angular steel plate screwed to both the upper or lower soleplate (or horizontal members) and vertical member.

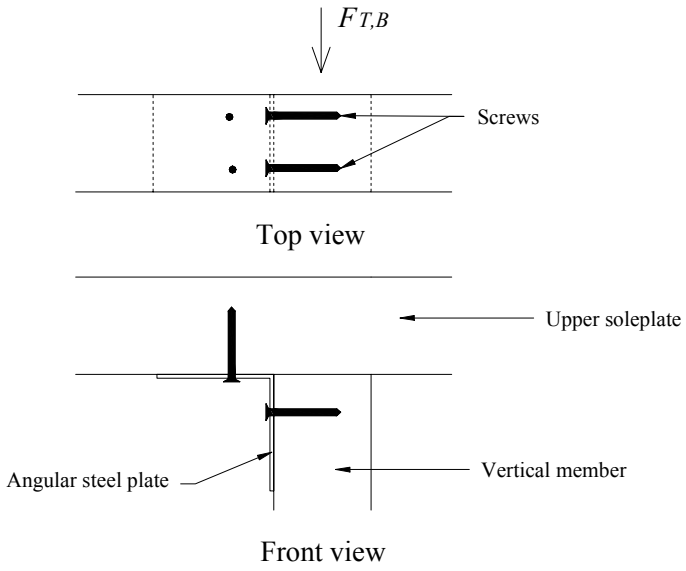

Figure 2-4 Top and bottom connections for vertical members.

For 35 mm long screws with 4 mm in diameter and a 2 mm thick steel plate, the maximum reaction force $F_{T,B}$ that could be taken is 1750 N considering two screws per shear plane (see appendix F, section F.1). The reaction force in the vertical members is given by:

$$F_{T,B} = pL/2 \qquad \textbf{(2-4)}$$

Substituting $F_{T,B}$ = 1750 and L = 2500, a value of p = 1.4 kN/m is found. This capacity is slightly higher than the calculated capacity of the vertical members (see previous section).

2.5 Upper soleplate and its connections

The lower soleplate is anchored to the foundation. Half of the load acting perpendicular to the panels would be transmitted by the vertical members to the lower soleplate through the bottom connections and from the soleplate to the foundation via the anchors. On the other hand , the upper soleplates transmit the other half and the roof load to the panels parallel to the force by bending. The considered soleplates would be 2500 mm long and 75x50 mm in section. These ones could be analyzed as simply supported beams with a concentrated load in the center produced by the top connections (when panel C of Figure B-2 in appendix B is used) or with uniform distributed load produced by the nails that join the horizontal members to the

soleplates (when panel A or B of Figure B-2 in appendix B is used). The worst case is when the concentrated load is assumed since the bending moment m_y is twice as the one produced by the uniform distributed load. The model is shown in Figure 2-5. The concentrated load in the center will be $2F_{T,B}$ (which is two times the reaction force of the vertical members because two top connections occur at that point) plus $F_{T,B}$ considering the roof load contribution. From Figure 2-5:

$$m_y = (3F_{T,B})L/4 \qquad \textbf{(2-5)}$$

Combining equations 2.3, 2.4 and 2.5:

$$p = \frac{4h^2 b\sigma_y}{9L^2} \qquad \textbf{(2-6)}$$

Taking the values h = 75, b = 50, σ_y = 20 and L = 2500, a value of p = 0.4 kN/m can be found. Transforming this capacity to a load per area, a value w = 0.4/0.625 = 0.64 kN/m^2 is obtained. This capacity is lower than the wind load according to IBC 2000 (1.1 kN/m^2). If panels A or B are used, the capacity will be twice (1.3 kN/m^2) and 1.2 times higher than the wind load calculated in section C.1.

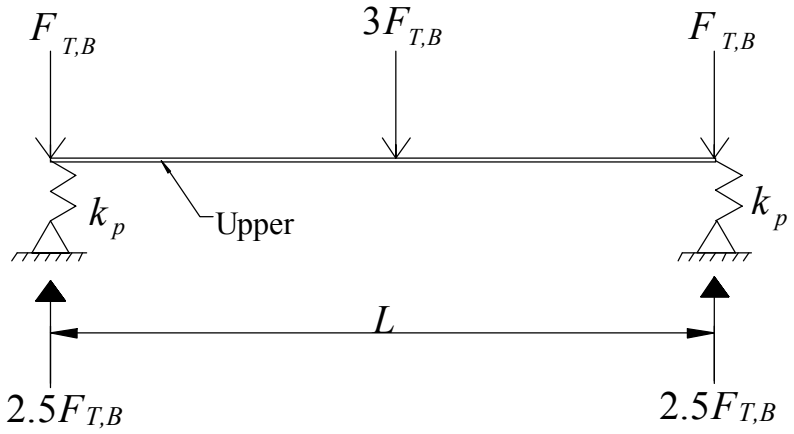

Figure 2-5 Upper soleplate model.

The connections between the soleplates could be made by using steel plates as shown in Figure 2-6. There would be two types of connections for the upper soleplate:

1. Connection between three soleplates (Figure 2-6a).
   Consists of two parallel soleplates (1 and 2) that meet at their ends and a soleplate parallel to the load that is part of a shear wall. The principle here is that the soleplate which has no direct support from the shear wall (2) is able to transmit its reaction. This could be achieved by nailing or screwing a steel plate to both parallel soleplates. The two reaction forces would be transmitted to the shear wall by compressing the soleplate parallel to the load. The connection must be able to transmit a load equal to $2.5F_{T,B}$.

2. Connection between two soleplates (Figure 2-6b).
   This case would occur in the corners and is the same principle as the previous one. The reaction force would be transmitted by the steel plate connection to the soleplate parallel to the load and then to the shear wall. The connection must be able to transmit a load equal to $2.5F_{T,B}$ as well.

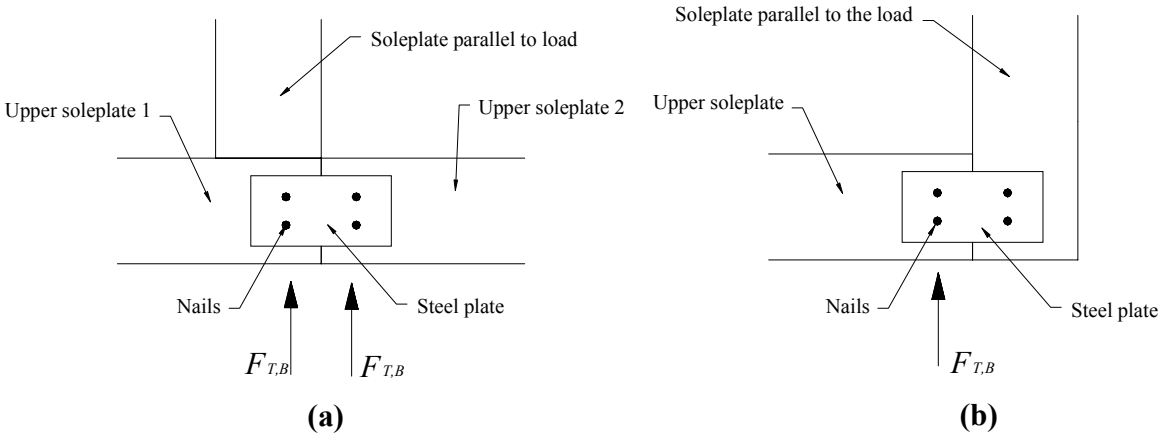

Figure 2-6 Connections between soleplates.

2.6 Resistance to lateral load (Shear walls)

The shear walls will be in charge of transmitting the lateral loads to the foundation. In the structural analysis there are two important features to consider:

1. Connection between sheet and frame.
2. Connection between panel (sheet and frame) and foundation (uplifting).

The previous is supposing that no lateral buckling will occur.

2.6.1 Connection between sheet and frame

Figure 2-7 shows a shear-wall composed by a wooden frame (two vertical and two horizontal members) and a plybamboo sheet. A relation between *R* (capacity of the panel to resist lateral load) and the maximum force in the maximum loaded nail can be calculated [4]. The model used to make this calculation assumes linear elastic behavior of the fasteners, hinged connections between individual elements and that uplift is prevented (see 2.6.2). Besides, the beam elements as well as the sheathing are considered to be completely stiff against bending and elongation in the loading plane.

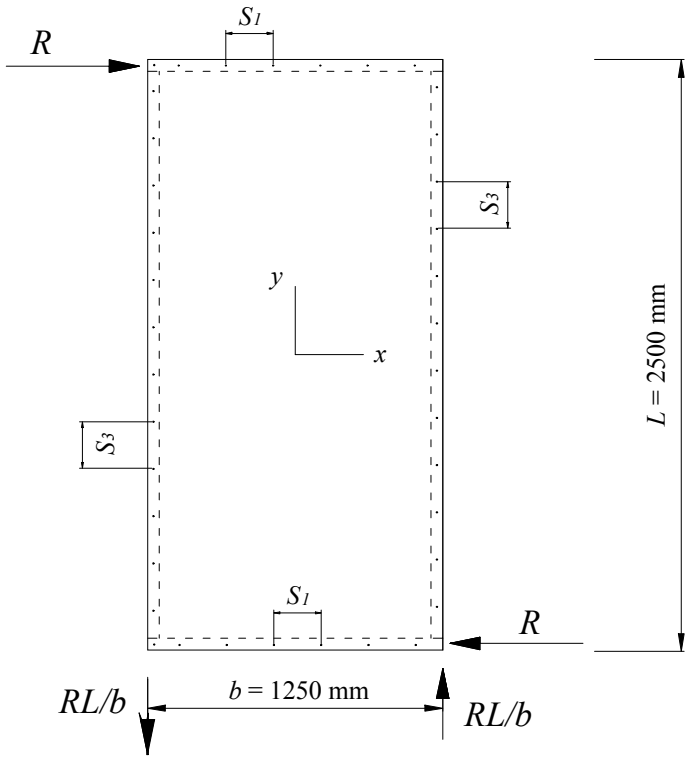

Figure 2-7 Plybamboo panel acting as a shear-wall.

With the assumptions previously mentioned, the following equations are developed:

$$F_{x,i} = \frac{R\ Ly_i}{\sum y_i^{\ 2}} \qquad \textbf{(2-7)}$$

$$F_{y,i} = \frac{RLx_i}{\sum x_i^{\ 2}} \qquad \textbf{(2-8)}$$

$$F_i = \sqrt{F_{x,i}^{\ 2} + F_{y,i}^{\ 2}} \qquad \textbf{(2-9)}$$

Where $F_{x,i}$ and $F_{y,i}$ are the force components in x- and y- directions respectively (the coordinates system is located at the center of the panel) for a fastener in position (x_i , y_i). F_i is the total force for a fastener i, L is the length of the wall unit and R is the capacity of the shear-wall.

Knowing that the nails are spaced every 150 mm, the lateral capacity of the wall can be obtained as follows:

$s_1 = s_3 = 150\,\text{mm}$ (Figure 2-7).

$$\sum x_i^{\ 2} = 17x2x600^2 + 4\left(150^2 + 300^2 + 450^2 + 600^2\right) = 14.94x10^6\,\text{mm}^2.$$

$$\sum y_i^2 = 9x2x1225^2 + 4\begin{pmatrix}150^2 + 300^2 + 450^2 + 600^2 + \\ 750^2 + 900^2 + 1050^2 + 1200^2\end{pmatrix} = 45.37x10^6\,\text{mm}^2.$$

$$F_{x,i} = \frac{2500x1250R}{45.37x10^6} = 0.069R\,,\; F_{y,i} = \frac{2500x625R}{14.94x10^6} = 0.104R$$

$$F_i = \sqrt{(0.069R)^2 + (0.104R)^2} = 0.125R \Rightarrow R = 8.0F_i$$

For a 2.8 mm diameter nail, 55 mm long:

F_i = 675 N (see appendix F, section F.2) $\Rightarrow R = 8x675 \Rightarrow R$ = 5400 N.

The required lateral capacity is 3.1 kN for seismic load (see section C.2 in appendix C) and 4.3 kN for wind loads ($5F_{T,B} = 5pL/2$ and p = 1.1x0.625 = 0.6875), so the nails can be spaced wider:

With $s_1 = s_3 = 200$ mm,

$\sum x_i^2 = 13x2x600^2 + 4(200^2 + 400^2 + 600^2) = 11.6x10^6$ mm^2.

$\sum y_i^2 = 7x2x1225^2 + 4(200^2 + 400^2 + 600^2 + 800^2 + 1000^2 + 1200^2) = 35.6x10^6$ mm^2.

$$F_i = \sqrt{(0.088R)^2 + (0.135R)^2} = 0.161R \Rightarrow R = 6.2F_i$$

For a 2.8 mm diameter nail, 55 mm long:

F_i = 675 N $\Rightarrow R = 6.2x675 \Rightarrow R$ = 4180 N < 4300 N required for wind loads.

2.6.2 Connection between panel and foundation

The connection between the panel and the lower soleplate must be able to take shear and moment forces to avoid uplifting of the panel. Figure 2-8 shows this connection for panel type A (see Figure B-2 in appendix B). Assuming a forced center of rotation (where the center point of the x-y coordinates axis is located), the group of fasteners would have to transmit a withdrawal vertical force whereas the vertical member on the right would be in compression to balance the vertical forces. The fasteners will also have to transmit shear forces.

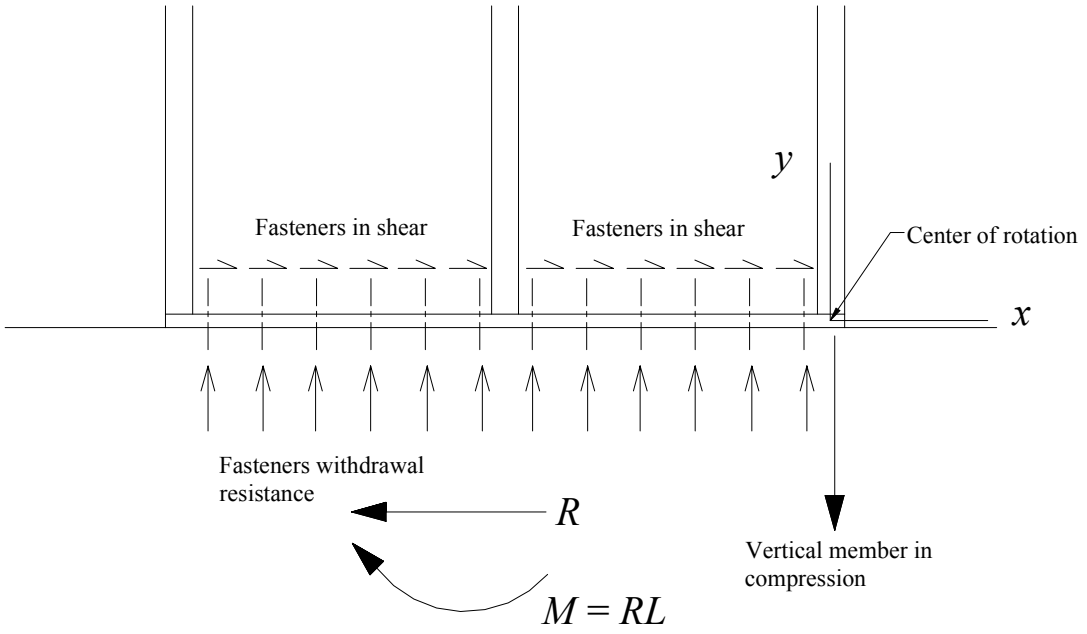

Figure 2-8 Panel bottom anchorage.

If small deformations are considered, the relationship between the forces and the displacements of the nails may be assumed linear. With this assumption, the following equation can be derived:

$$F_i = \frac{Mx_i}{\sum x_i^2} \qquad \textbf{(2-10)}$$

Where,
F_i: force for a fastener *i*.
$M = RL$: external bending moment (L is the panel length).
x_i: distance of fastener i to the center of rotation.

Equation (2-10) can be rewritten as:

$$R = \frac{F_{\max} \sum x_i^2}{L x_{\max}} \qquad \textbf{(2-11)}$$

Where,

F_{max}: maximum force for a fastener *i*.
x_{max}: maximum distance from a fastener *i* to the center of rotation.

Using 12 screws of 4.9 mm diameter and 49 mm long spaced each 100 mm, the lateral capacity of the panel can be calculated. The withdrawal capacity of these screws will be approximately 1130 N (see appendix F, section F.3). Hence,

$$\sum x_i^2 = 75^2 + 175^2 + 275^2 + 375^2 + 475^2 + 575^2 + 675^2 + 775^2 + 875^2 + 975^2 + 1075^2 + 1175^2 = 6117500 mm^2$$

$$R = \frac{1130 x 6117500}{2500 x 1175} = 2350 \text{ N.}$$

It can be calculated that the vertical element on the right would be submitted to a compression force of approximately 9500 N[1]. The design buckling resistance of such member is around 7900 N (see appendix F, section F.4). However, the vertical members are restricted laterally by the panels on their sides which will considerably increase the buckling resistance.
In the case of panel B, the horizontal member could be just nailed to the lower soleplate because the sheet is laterally joined to the lower soleplate (see Figure B-3 in appendix B). In both panels B and C, the lower soleplate is well anchored by the steel bars coming from the foundation.

2.7 Suction

The expected suction load on one plybamboo sheet would be 1.5 kN/m^2 (see Figure C-1 in appendix C). The total area of one sheet is 2.5x1.25 = 3.125 m^2. The screws would be then submitted to a total load of 1.5x3.125 = 4.7 kN. If the spacing of the screws is 200 mm, 24 of them would be holding the sheet which means that they must resist a load of 4.7/24 = 0.2 kN. The withdrawal capacity of the screws is 2.0 kN (see section F.3 in appendix F), thus more than sufficient.

[1] Sum of the forces in the 12 fasteners which can be calculated with equation 2-10.

2.8 Conclusions

Table 2-1 shows a summary of the most important results obtained in the different sections of chapter 2. The following are the most relevant conclusions from the chapter:

Using theory of plates, it can be calculated that the capacity of a plybamboo sheet (of 2500x1250x12 mm simply supported along its four edges) to resist bending in its perpendicular direction is 5.4 kN/m^2 which is 4.9 times higher than the expected load produced by a wind pressure of 1.1 kN/m^2 (section 2.2).

Full-scale tests of these sheets submitted to perpendicular load must be carried out in order to see how accurate the theoretical model is and also to obtain the stiffness of such element (deflection control).

Vertical wood members of 2400x75x50 mm and a design bending strength of 20 N/mm^2 have a capacity of 1.2 kN/m (1.9 kN/m^2 when divided by the tributary width of 0.625 m) when simply supported and submitted to a uniform distributed load, which is 1.7 times higher than the expected load produced by a wind pressure of 1.1 kN/m^2 (section 2.3).

In the future, laminated bamboo beams may replace these vertical elements and probably the section could be smaller because of the higher strength and stiffness. In places where the conditions are not as severe as the considered ones, the section and strength of the vertical members could be reduced after checking that the new member is capable of resisting the imposed actions.

In the structural analysis example, the capacity of the top and bottom connections is in the same range (1.0-1.5 kN/m) than the capacity of the vertical members. The advantage of this connection is that its capacity could be increased or decreased by using more or less fasteners or by changing their length and/or diameter (section 2.4).

When using panel type C (Figure B-2 in appendix B), the capacity of the upper soleplate of 2500x75x50 mm and 20 N/mm^2 of design bending strength is 0.64 kN/m^2 which is not enough to resist a wind load of 1.1 kN/m^2. In order to withstand such wind load, the strength must be at least 35 N/mm^2 which is a common design value for hard woods. Nevertheless, the nailed connections would be more difficult to achieve (see section 2.5).

When using panel type A or B (Figure B-2 in appendix B), the capacity of the previously mentioned upper soleplate would be 1.2 times higher than the required wind load in the example (appendix C).

In general, panel type C is only recommendable in zones where the wind or seismic loads are not as high as the ones presented in the example; panel type A and B could be implemented in places where high wind or seismic loads are expected.

The connections between the soleplates could be achieved in the same way as for the vertical members.

The lateral capacity of one panel using nails spaced every 200 mm is 4.2 kN according to the theoretical calculations. The required capacity according to the example is 4.3 kN for wind loads and 3.1 kN for seismic loads in one shear wall. However, at least two complete panels (without windows nor door openings) would compose a shear wall and hence, the capacity would increase considerably (see section 2.6.1). When panel type A is used, the lateral capacity of one panel decreases to 2.4 kN (see section 2.6.2). That is why it is only recommendable to be applied in zones where the wind or seismic loads are not as high as the ones presented in the example (appendix C).

Full-scale tests on lateral capacity including window openings of certain size must be carried out in order to compare the results with the theoretical calculations.

The wind suction phenomena will not be a problem for the sheets according to the theoretical calculations (see section 2.7).

Table 2-1 Summary of results of chapter 2.

Section	Item	Strength	Load (appendix C)
2.2	Sheets in bending	5.4 kN/m^2	1.1 kN/m^2
2.3	Vertical members	1.9 kN/m^2	1.1 kN/m^2
2.4	Top and bottom connections	2.2 kN/m^2	1.1 kN/m^2
2.5	Upper soleplate with panel type C	0.64 kN/m^2	1.1 kN/m^2
	Upper soleplate with panel type A or B	1.3 kN/m^2	1.1 kN/m^2
2.6	Shear walls, sheet to frame connection	4.2 kN/panel	4.3 kN/shear wall
	Shear walls, panel to foundation connection	2.4 kN/panel	4.3 kN/shear wall
2.7	Suction	2.0 kN/screw	0.2 kN/screw

3 CORNER CONNECTION

3.1 Introduction

This chapter deals with experimental tests for corner connections for the house design method using plybamboo sheets. The design method (see appendix B) consists of two possible corner connections (see Figure B-1) in a house which are shown in Figure 3-1. Corner connection 1 would be most commonly used. Corner connection 2 may also be used in cases where the house has five external corners or for some internal walls. This report concentrates on corner connection 1.

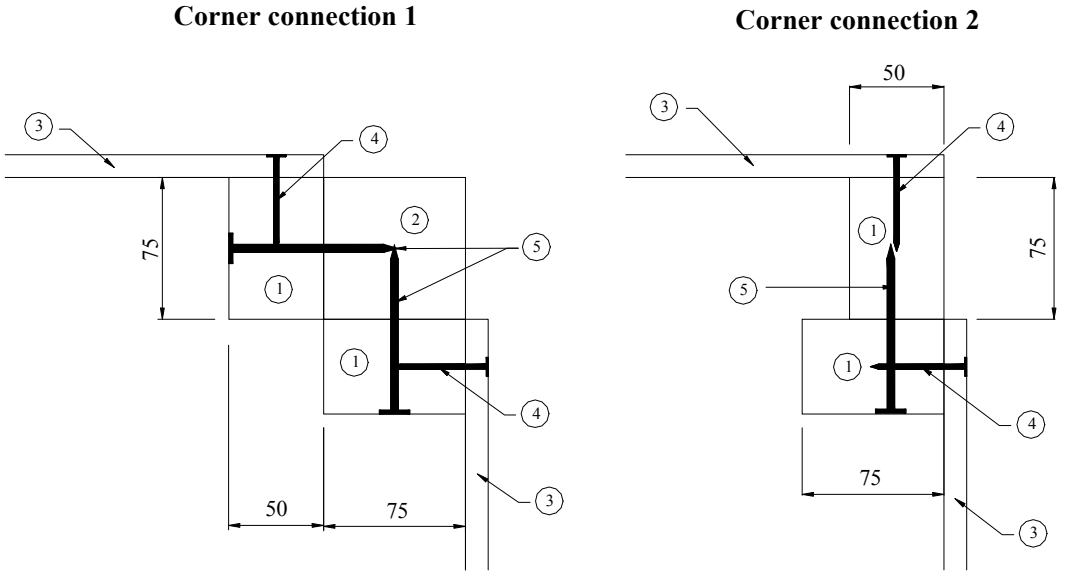

1. 75x50 mm wood piece
2. 75x75 mm wood piece
3. Plybamboo sheet (12 or 18 mm thick)
4. 2.8 mm diameter nail (3 is predrilled)
5. 4.1 mm diameter nail (1 is predrilled)

Figure 3-1 Top view of the possible corner connections in the design method.

The purpose of the tests is to obtain the structural capacity of these corner connections. Knowing the capacity, design of such corners to withstand wind loads and earthquakes could be possible.
In order to analyze the structural behavior of this connection, part of the whole connection is modeled (see Figure 3-2). The size of the model is shown in Figure 3-2a. The width is taken as 625 mm which is half of the sheet width. The length of 450 mm is related to the spacing of the nails or fasteners used to join the vertical members to the sheets. With a spacing of 150 mm, three fasteners are needed to build the model.
The horizontal wind or seismic forces are modeled as a resultant force acting along the length of the horizontal member of the model (Figure 3-2b). One of the advantages of the previous model is that it can be analyzed as a two-dimensional structure (see Figure 3-2c).
After all these considerations, the corner connection model was built and tested. The test setup is described in section 3.2. Details of the construction of the model are also shown (section 3.2.1). This includes how the specimen was put together and mounted on a steel frame. Besides, descriptions of the supports are presented as well.

In section 3.2.2 the loading procedure and the deformation measurement system are explained.
Before test series were performed, an exploratory phase (section 3.3) was carried out in order to understand the structural behavior of the model. This phase included three experiments and the difference between them was the way in which the plybamboo sheets were joined to the 75x50 mm wood pieces. The first one was joined using only nails as shown in Figure 3-1 . The second one was joined using glue in combination with nails and the last one was joined using only screws instead of nails.

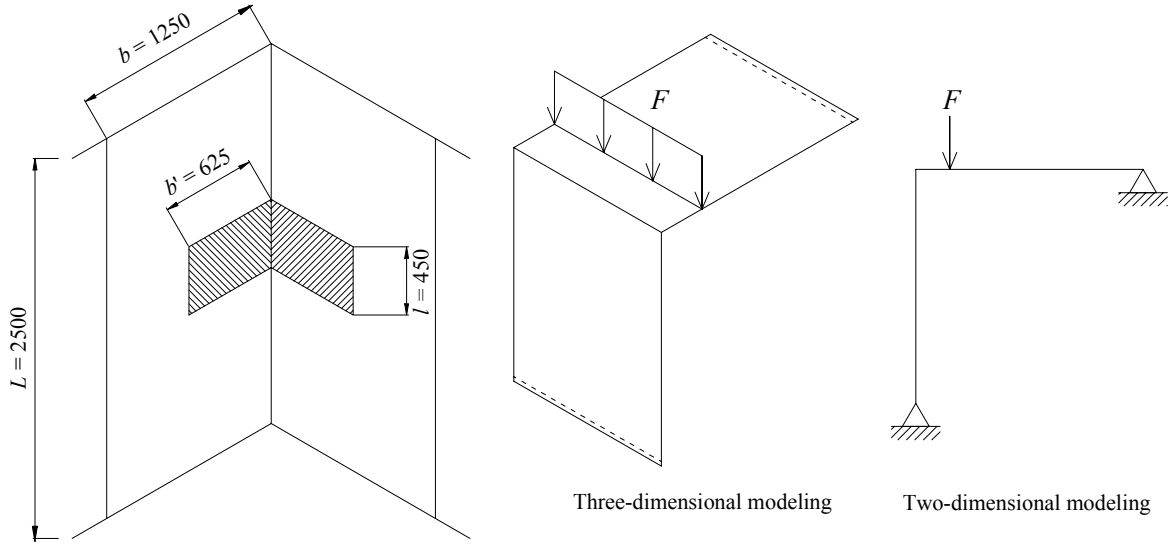

Figure 3-2 (a) Corner connection showing the part to be modeled. (b) Three dimensional modeling of the corner connection. (c) Two dimensional modeling of the corner connection.

A comparison between the structural behavior of these three tests is also presented. The exploratory phase demonstrated that the best way to join the plybamboo sheets to the vertical members is using screws. This is due to the fact that the withdrawal capacity of screwed joints is much higher (in the range of five times depending on properties such as fastener diameter and wood density) than that one of nailed joints. The previous lead to perform test series using screwed joints (section 3.4). Three tests were performed using bamboo mat boards (12 mm thick) and three using bamboo strip boards (18 mm thick). Experimental results and analysis are included in section 3.4.
To complement the experimental results, a theoretical explanation of the structural behavior of the corner connection is presented in section 3.5. The analysis is based on the failure modes observed during the tests, theoretical capacities of the joints (Appendix D) and equilibrium equations corresponding to the connection.
Finally, conclusions are given in section 3.6.

3.2 Experimental setup

In order to fixate the model for the corner connection a steel frame was built. This frame is useful for the structure supports and the placing of the dial gages and load cells. The frame offers an independent fixed reference system for measurement of displacements.

3.2.1 Specimen and frame

Figure 3-3 and Figure 3-4 show how the specimen and steel frame were built. The specimen is composed by one 75x75x450 mm wood piece (2), two 75x50x450 mm wood pieces (1) and two 12(18)x625x450 mm plybamboo sheets (3). The specimen is joined together as seen in detail 3 of Figure 3-4.

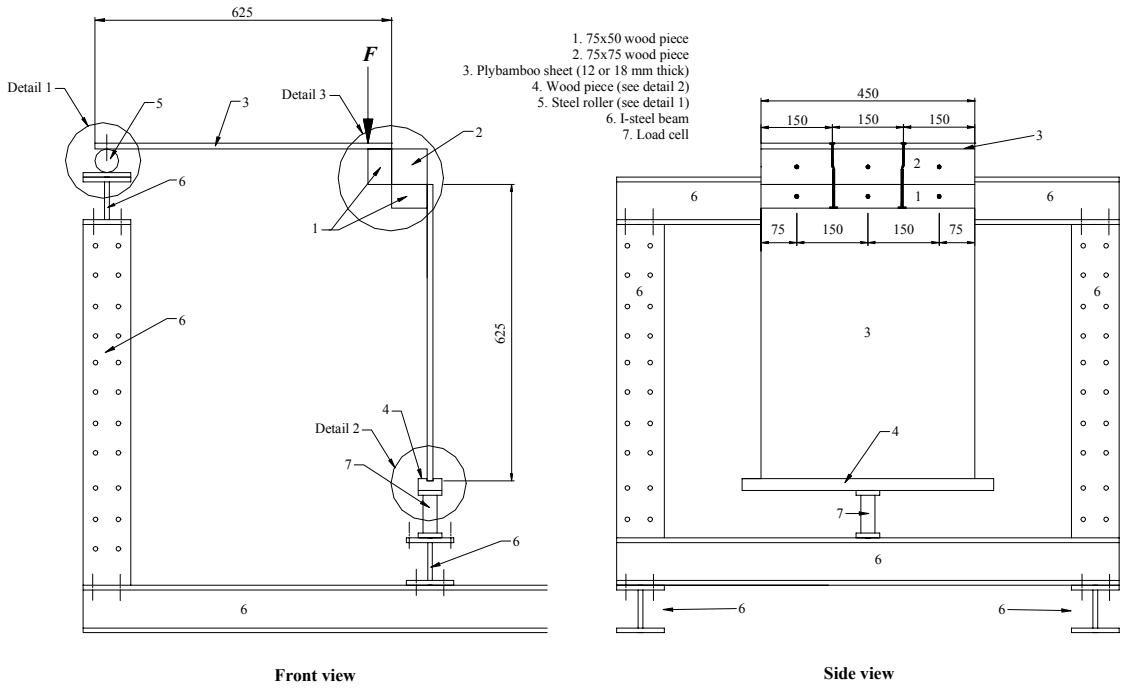

Figure 3-3 Test setup showing specimen and frame.

In the case of nail 1, only the plybamboo sheet (3) is predrilled whilst in the case of nail 2, only the 75x50 mm wood piece (1) is predrilled.
Elements 1 and 3 represent the prefabricated panel whereas element 2 represents the vertical element placed and joined on site. The used wood corresponds to K24 class B which is a soft wood with a bending characteristic value of 24 N/mm^2 and a mean density of about 490 kg/m^3.
The support for the horizontal sheet is shown in detail 1 of Figure 3-4.
It consists of a steel roller (5) joined to a steel plate on the extremes. This roller is able to rotate around its longitudinal axis. The sheet is fastened to the roller so that when the load is applied it can rotate.
The bottom support is shown in detail 2. The plybamboo sheet rests on a wooden piece with a small channel (4). This allows the rotation of the sheet. Wooden piece 4 is supported by one load cell (7) in order to measure the load transmitted by the corner connection.

The steel frame is composed by wide flange H-beams (6) and its function is to support wood piece (4) and the steel roller (5).

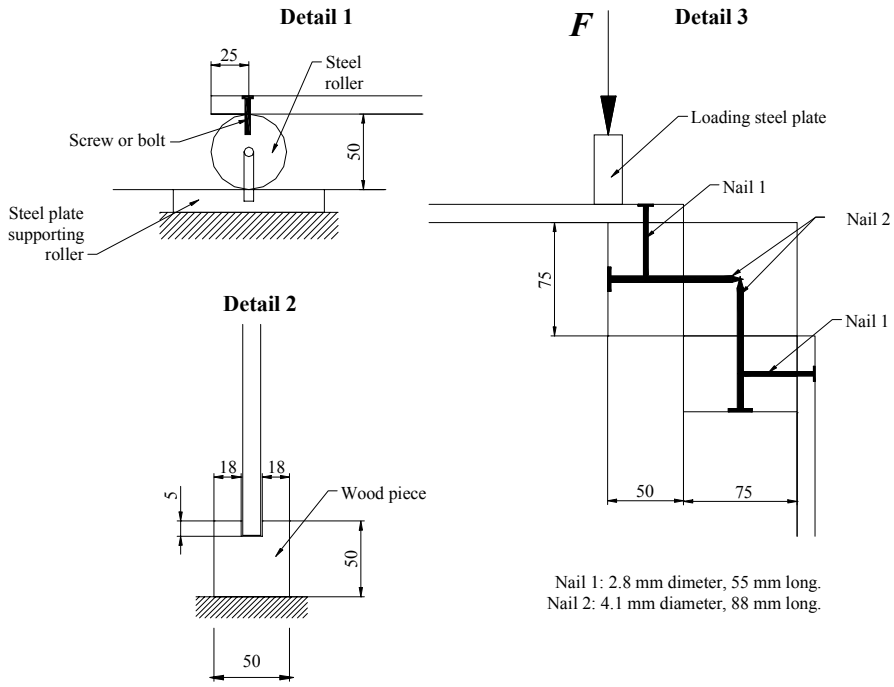

Figure 3-4 Supports and connection details.

3.2.2 Measurement of load and deflection

The loading system consists of two hydraulic jacks and a load cell. One jack (the controlling one) is placed in a compression machine (see green circle in Figure 3-5). The other one (the loading one) is placed above the specimen and is held by an upper H-beam (see yellow circle in Figure 3-5). The two jacks are connected by an oil pressure tube (see red arrow in Figure 3-5) which transmits the pressure applied to the jack on the compression machine to the one above the specimen. The advantage of doing so is that the displacement is controlled by the speed system of the compression machine. A load cell is placed under the specimen (see blue circle in Figure 3-5) to measure the load transmitted by the connection as previously explained. The load was measured every 5 seconds at a speed rate of 1 mm/min. The loading procedure is explained in Table 3-1 and further complemented by Figure 3-6 for better understanding.

Table 3-1 Loading procedure during tests.

Step / Measurement*	*Compression machine*	*Load cell*	*Deformations*
1.Placing the specimen	0	Part of specimen	0
2.Pulling Jack	Jack weight 1	Part of specimen	0
3.Placing loading plate	Jack weight 1	Part of (specimen + plate)	Yes
4.Pushing Jack	0	Part of (specimen + plate + jack 2)	Yes
5.Loading at 1 mm/min	Increased load	Increased load	Yes

*See also these numbered steps in Figure 3-6.

It could be summarized as follows:

1. When the specimen is placed, only the load cell will measure load. This load would be equal to certain percentage of the specimen weight.
2. Afterwards, both jacks must be pulled up in order to make room for the loading steel plate. At this moment, part of the jack weight in the compression machine and part of the jack weight above the specimen is read on the compression machine (Jack weight 1 in Table 3-1 and Figure 3-6). The load cell will be still reading the specimen weight. The deformation system is turned on and starts to measure.
3. The loading steel plate is placed on the specimen. The compression machine will be still reading the Jack 1 whereas the load cell would read certain percentage of the specimen and steel plate weight. At this moment, deflections are measured.

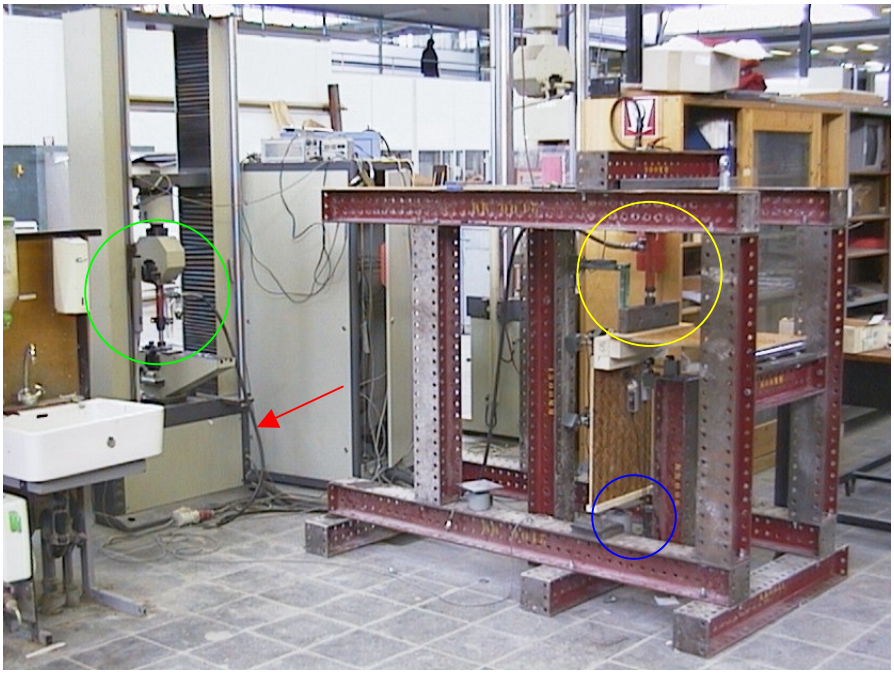

Figure 3-5 Experimental setup showing loading system.

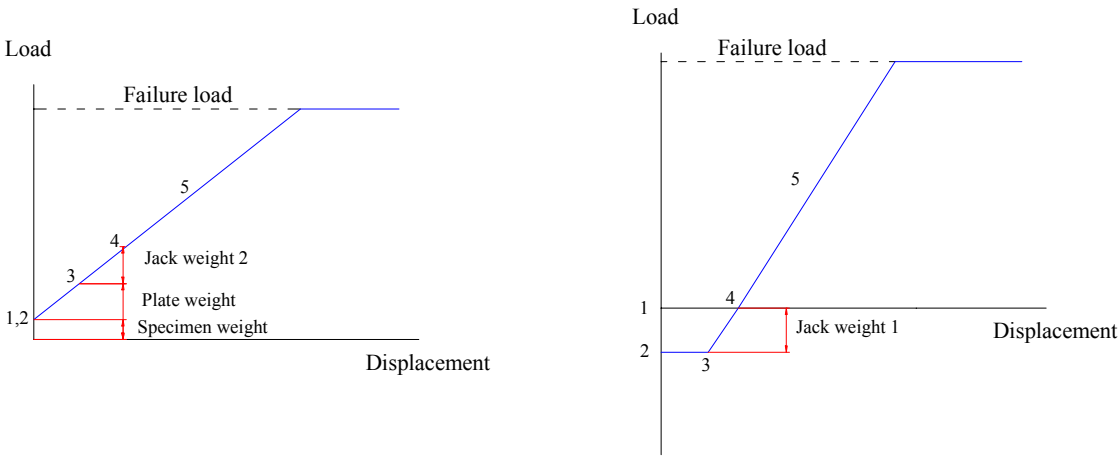

Load-displacement curve for load cell **Load-displacement curve for compression machine**

Figure 3-6 Expected load-deflection curves for load cell and compression machine.

4. The jack on the compression machine is pushed until the jack above the specimen has reached the loading steel plate. At this time, the compression machine would read approximately zero whereas the load cell will read part of the jack weight that is above the specimen (Jack 2 in Table 3-1 and Jack weight 2 in Figure 3-6).
5. Finally, the compression machine begins to push the jack at a speed rate of 1 mm/min.

The deflection measurement system consists of 5 digital dial gages placed on different positions on the specimen. Figure 3-7a shows a scheme in which each deflection is numbered and Figure 3-7b shows a photograph of the actual test setup. Dial 0 measures the horizontal displacement at the center of the vertical sheet. 1 and 2 measure horizontal displacements with the purpose to obtain the rotation of the 75x75 mm piece. Dial gages 3 and 4 measure vertical displacements of the two 75x50 mm pieces. All these dial gages as well as the load cells are connected to a computer. Hence, the computer reads 7 measurement channels including the compression machine which regulates the loading speed of 1 mm/min.

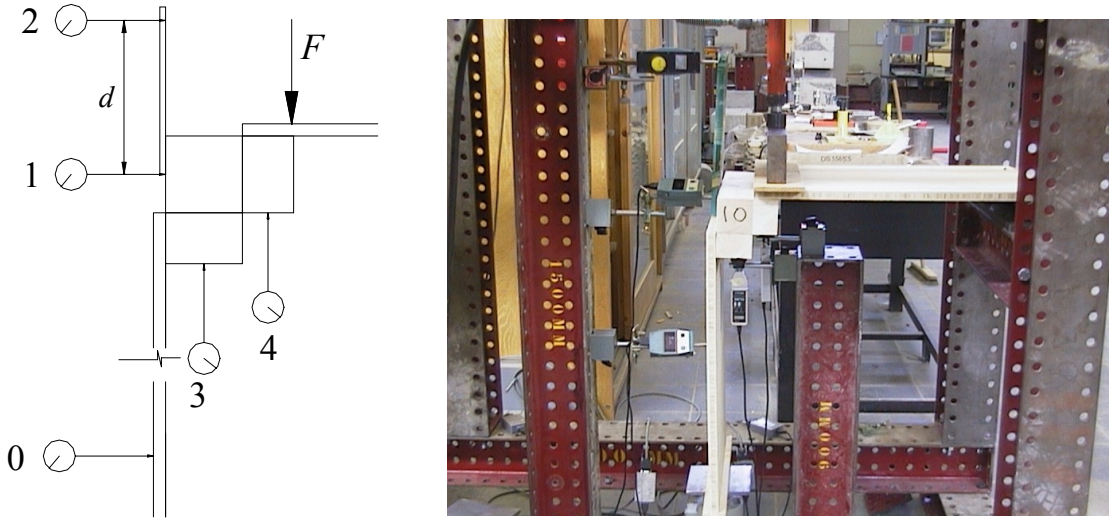

(a) (b)

Figure 3-7 (a) Deflection measurement system scheme. (b) Test setup showing the deflection measurement system.

3.3 Exploratory phase

This section describes three different tests for the corner connection. The first one is a nailed connection as shown in detail 3 of Figure 3-4. The second is the same as the first one but gluing the plybamboo sheets to the wooden elements. The connection wood-to-wood is not glued. The third and last one is a screwed connection. 4.9 mm diameter and 49 mm long screws replace the nails (1) in detail 3 of Figure 3-4. The connection wood-to-wood remains the same.

Note: The capacity of the load cell used for these three tests was 2 kN. Hence, the load-deflection curves were measured until 2 kN (See Figure 3-11). The three tests were done using bamboo mat boards.

3.3.1 Nailed test

The first corner connection test was done using nails for joining the sheet-to-wood and wood-to-wood connections just as shown in detail 3 of Figure 3-4.
The ultimate failure load (read by the load cell) for this test was around 500 N (see blue curve in Figure 3-11).
The load read by the load cell on the bottom was 70% of that one read on the compression machine. It seemed that the bending moments in B1 and B4 were causing the withdrawal of the nails joining the sheets and the wood (see Figure 3-8). The moment capacity of B1 and B4 is so small that with a small load the connection becomes a mechanism where two hinges in B1 and B4 are produced. Figure 3-8 also shows that there is no failure in B2 and B3.

From this test it can be concluded that the corner connection becomes weak if only nails are used to join each of the members, especially the joints between the plybamboo sheets and the wooden members.

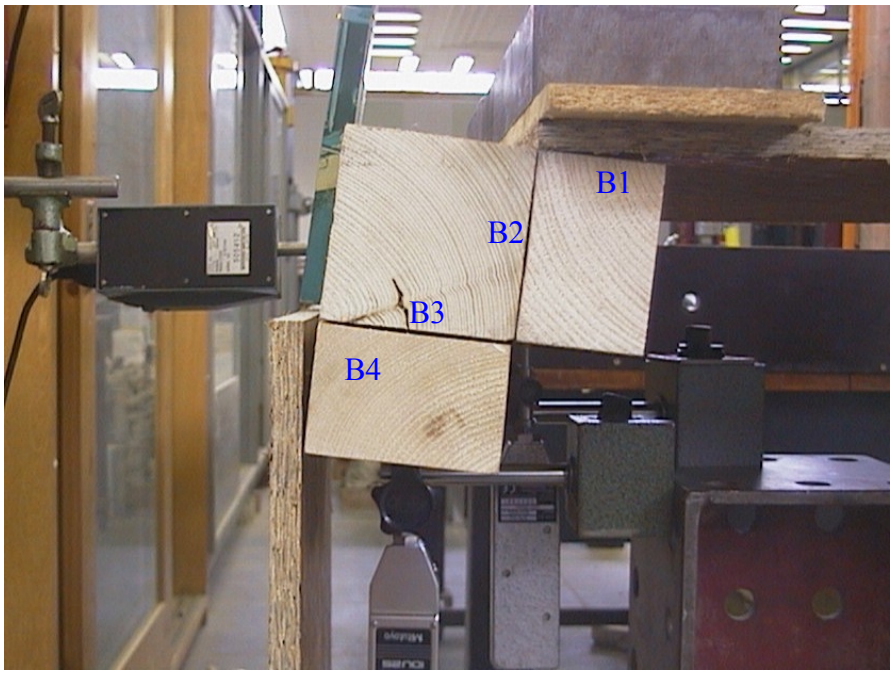

Figure 3-8 Failure in corner connection using only nails.

3.3.2 Glued test

As expected, the glued test connection was stronger than the nailed one (see green curve in Figure 3-11). The ultimate load was 2400 N (this load was derived from the maximum load registered by the compression machine and the relation between the previous readings of the load cell and compression machine) which is almost 5 times the obtained ultimate load for the nailed connection. The reason is that now, the moment capacities of B1 and B4 are much larger due to the glue. This time the load read by the load cell on the bottom was approximately 80% of that one read in the compression machine.

Observed structural behavior (see Figure 3-9):

1. At the beginning, both plybamboo sheets start to bend in their longitudinal direction (see Figure 3-9a).
2. The first crack appears in the vertical plybamboo sheet (see Figure 3-9b). This was probably due to tensional stresses perpendicular to the grain produced in the sheet. This effect can be noticed in the green curve of Figure 3-11 at around 1.7 kN.
3. An opening in B2 occurred. It appears that the moment capacities in B1 and B3 are larger than that one in B2. Hence, a withdrawal of the nail in B2 occurred (see Figure 3-9c).
4. Finally, the ultimate load is reached when the glue and part of the sheet are broken in B4 due to tensional loads produced by the moment in B4. At this

time, the opening in B2 was bigger than before. No failure in B3 was observed.

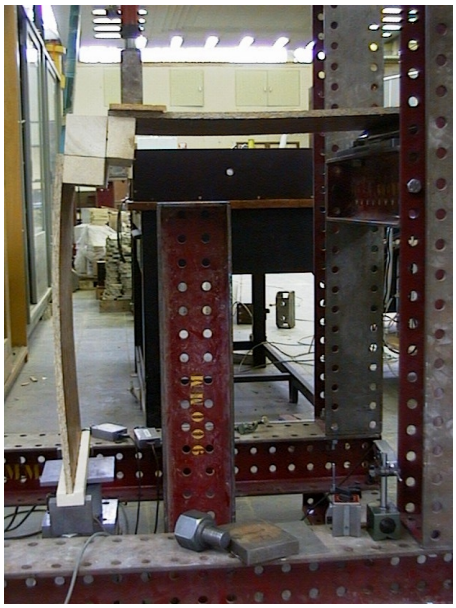

(a) Sheets begin to deform.

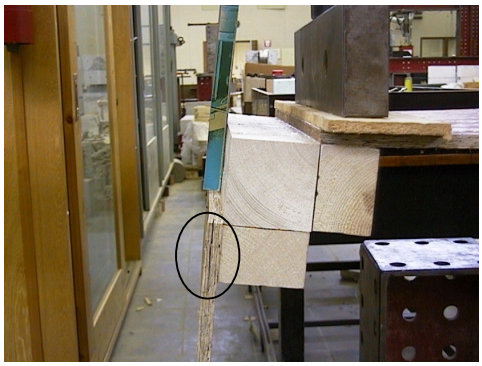

(b) First crack appears (delamination).

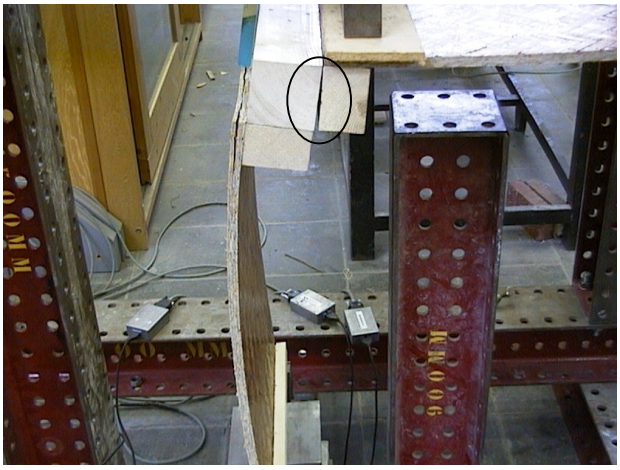

(c) Opening in B2.

(d) Failure in B4 and B2.

Figure 3-9 Observed structural behavior in corner connection using glue.

3.3.3 Screwed test

The screwed test was very similar to the glued test in terms of failure load and rigidity (see red curve in Figure 3-11). However, the observed structural behavior was quite different. The ultimate failure load was 2460 N (derived on the same way as for the glued connection test). The load read in the load cell on the bottom was approximately 80% of that one read in the compression machine. The previous confirms that the distribution of forces was quite the same compared to the one in the glued connection.

Observed structural behavior:

1. Both plybamboo sheets start to bend in their longitudinal direction.
2. Small openings start to appear in B1 and B4. The wooden pieces in B4 and B1 try to rotate but the screws do not allow this movement and hence the sheet (only the vertical one) starts to bend in its short direction as well. This effect can be clearly seen in Figure 3-10.
3. An opening in B2 occurs.
4. The ultimate load is reached and the connection cannot take more load (see Figure 3-10).

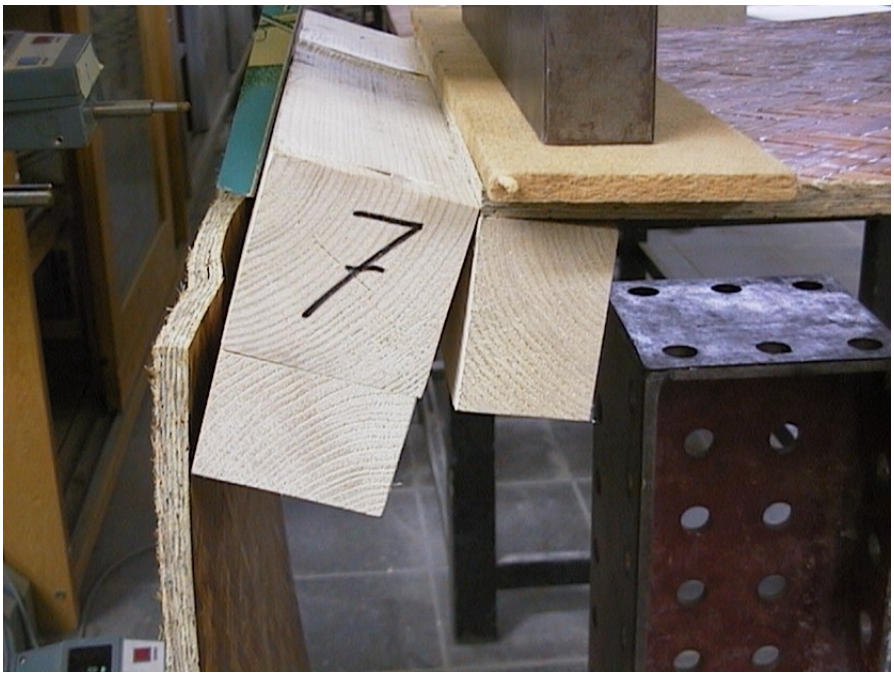

Figure 3-10 Failure in corner connection using screws.

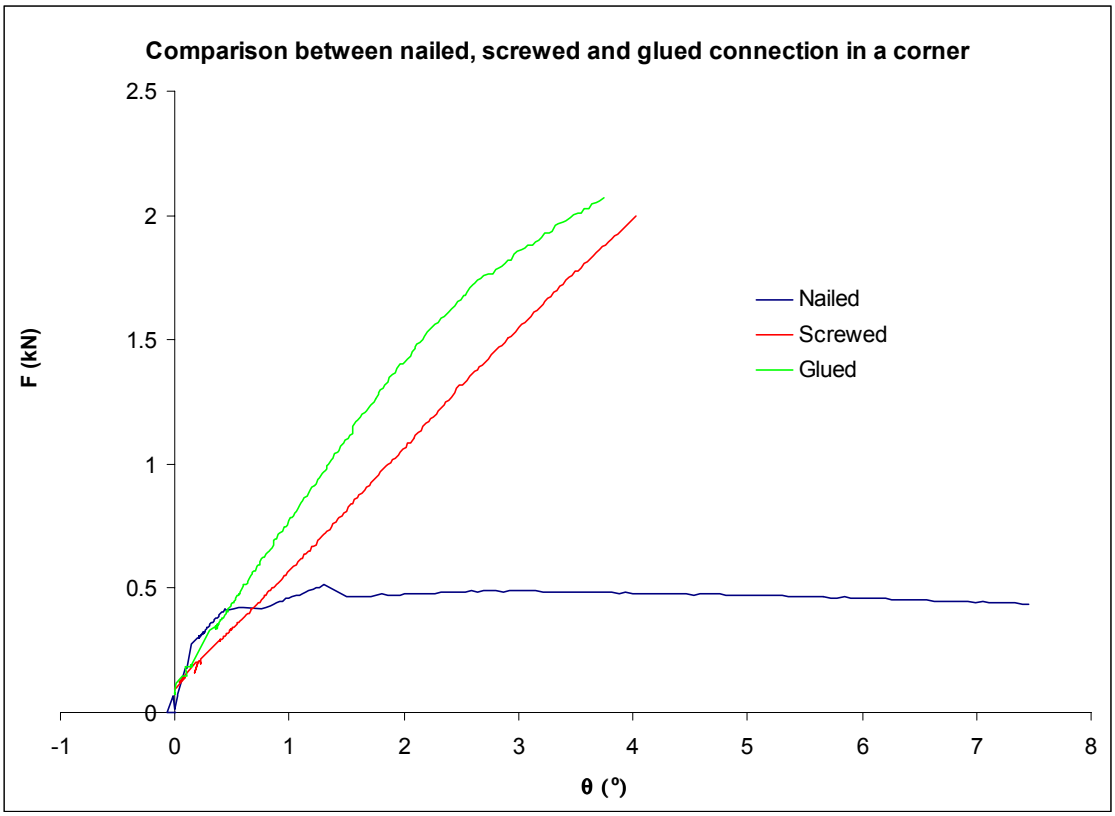

Figure 3-11 Load-rotation curves for nailed, glued and screwed tests with MB.

3.4 Test series and analysis

After the exploratory phase, test series were done on the screwed connections. 3 tests were done using bamboo mat boards (MB) and 3 using bamboo strip boards (SB). Table 3-2 shows a summary of the most important results for each of the tests.

Table 3-2 Test series results for the corner connection.

Test	F_y (N)	F_u (N)	θ_y (º)	δ_{0y} (mm)	F_{LC} / F_{CM}
MB1	1700	2600	3.5	10	0.79
MB2	3050	3200	8.4	19.9	0.79
MB3	3400	3600	9.3	24.9	0.80
SB1	3500	4300	2.8	5.9	0.84
SB2	3050	3950	3.4	6.0	0.83
SB3	2100	3800	2.1	3.0	0.80

In Table 3-2, five results for each test are shown (see Figure 3-12):

1. F_y indicates that the initial rigidity r_i will change and decrease.
2. F_u is the ultimate load or maximum load registered by the load cell.
3. θ_y is the rotation (of the 75x75 mm piece) read at F_y.
4. δ_{0y} is the horizontal deflection (at the center of the vertical sheet) read at F_y. See dial gage 0 in Figure 3-7.
5. F_{LC} is the force read in the load cell and F_{CM} is the force read in the compression machine. The previous was done by comparing the increase of the two forces in the same period of time. This time was taken in the straight part of the load-deflection curves (see Figure 3-6).

The rotation θ in degrees was calculated with the following equation:

$$\theta = \arctan\left(\frac{\delta_1 - \delta_2}{d}\right)\left(\frac{180}{\pi}\right)[º] \qquad \textit{(3-1)}$$

Where δ_1 and δ_2 correspond to the deflection read by dial gages 1 and 2 in Figure 3-7 respectively. d is the distance shown in Figure 3-7 (usually 300 mm).

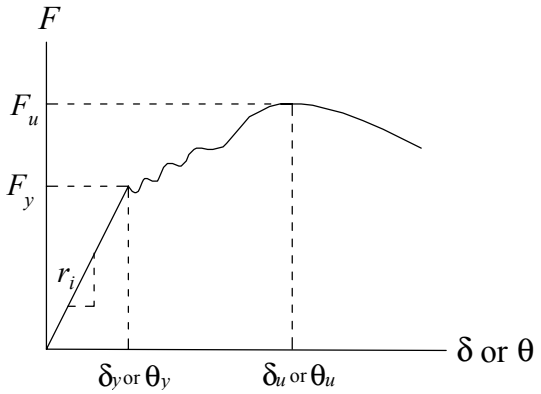

Figure 3-12 Load-displacement curve showing most important parameters.

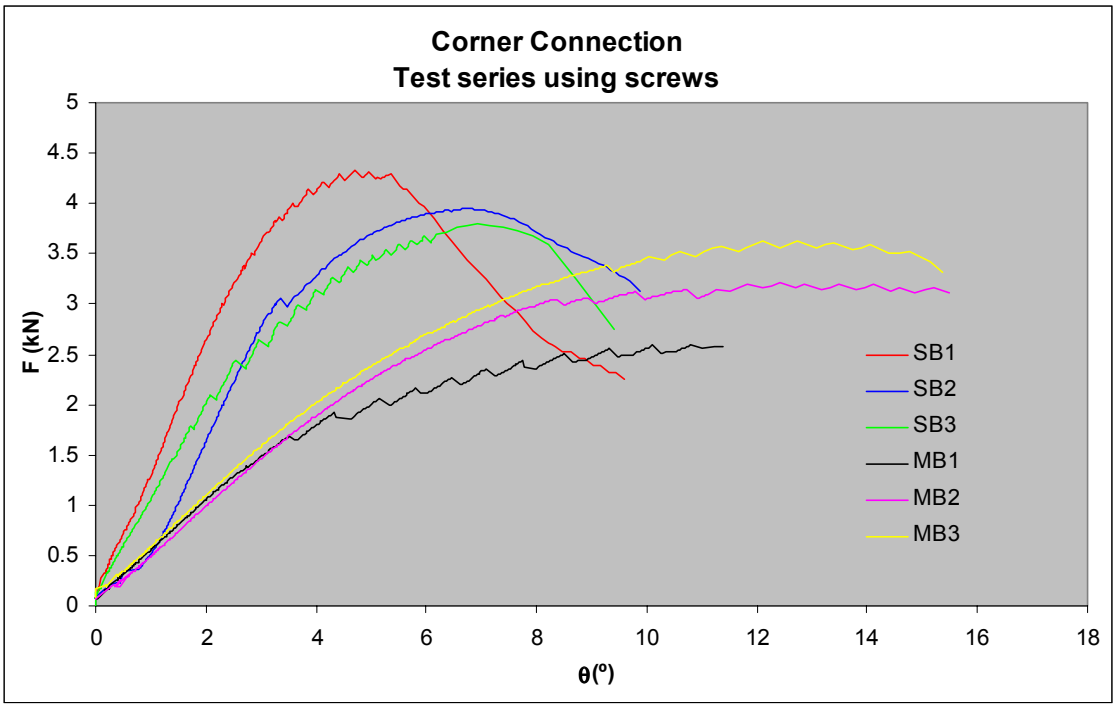

Figure 3-13 Load-rotation curves for test series using screws.

3.4.1 Test MB1

The structural behavior was the same as the one described in section 3.3.3. At approximately 1700 N, an opening in B2 appears. After this failure, the load is still increasing and decreasing in several steps as shown in the black curve of Figure 3-13 (MB1). This is due to the withdrawal of the nail. Every time the nail is pulled, a decrease in the load occurs and a moment later it increases again. It has to be noted that after the first withdrawal, the connection loses strength regarding the withdrawal capacity and consequently the moment capacity as well. The stiffness is then gradually decreasing. The connection reached its ultimate capacity when the load cell recorded 2600 N. The load cell read 79% of the load read in the compression machine.

3.4.2 Test MB2

The structural behavior is the same as the previous one. The main difference can be seen in the failure loads. The first stiffness loss was registered at 3050 N. Once more, the failure was due to the withdrawal of the nail at B2. The effect of the increasing and decreasing of the load can also be seen. However, the ultimate load was approximately the same as F_y (see pink curve in Figure 3-13). It is important to notice that between 2 and 2.5 kN, the load-deflection curve changes in slope which means that certain rigidity has been lost. The load cell read 79% of the load read in the compression machine.

3.4.3 Test MB3

The third test showed the same behavior as test MB2 although the connection was stronger (see yellow curve in Figure 3-13).

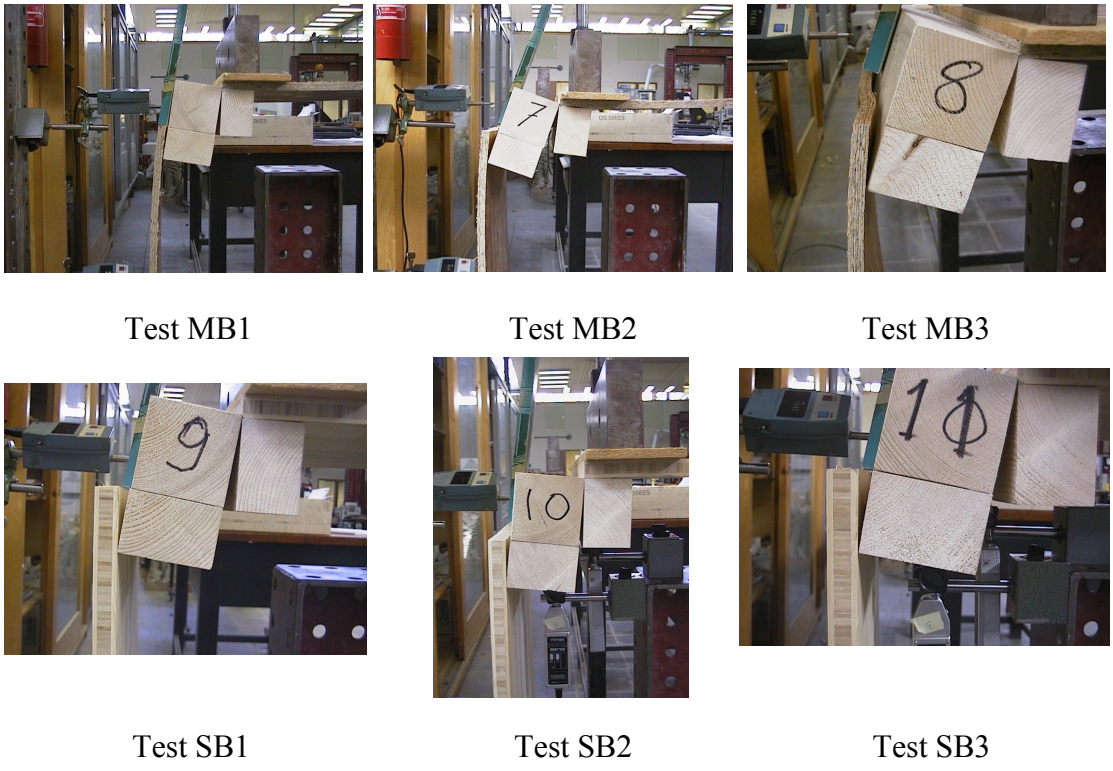

Test MB1 Test MB2 Test MB3

Test SB1 Test SB2 Test SB3

Figure 3-14 Failure modes in test series for screwed connections.

3.4.4 Test SB1

The behavior observed in the tests using bamboo strip boards was different to the ones using bamboo mat boards. The thickness and modulus of elasticity of the strip boards is larger than those ones for mat boards and hence the connection is stronger and stiffer.
The vertical sheet started rotating sideways instead of bending in its long direction. This makes the connection stiffer (see red curve in Figure 3-13). The first failure occurred in B2 (3500 N) due to the withdrawal of the nail and the effect of the increasing and decreasing of the load can be seen as well. However, the connection rapidly loses strength as shown in Figure 3-13 making it less ductile[2] than the connection using mat boards. This connection was the strongest of all with an ultimate failure load of 4300 N. The force read in the load cell was 84% of that one read in the compression machine.

[2] Ductility in this case is referred to as the capacity of the connection to deform from *Fy* to *Fu* (see Figure 3-12).

3.4.5 Test SB2

This test showed the same behavior than test SB1 (see blue curve in Figure 3-13). It can be seen that the rigidity was similar. In this test, the increasing and the decreasing of the load is not as visible as in test SB1 and SB3 and there is only one important rigidity change at 3050 N. The ultimate load was reached at 3950 N. The load cell read 83% of the load read in the compression machine.

3.4.6 Test SB3

This was the weakest of the tests using strip boards (see green curve in Figure 3-13). The connection is less rigid at the beginning. The joint in B2 began to fail at 2100 N. The decreasing and increasing of the load occurred until the ultimate load was reached at 3800 N. The load cell read 80% of the load read by the compression machine.

3.5 Structural behavior according to the experimental results

In this section, the structural behavior of the corner connection is explained. Theoretical calculations are presented for nailed and screwed connections and comparisons with the experimental results are discussed. The theoretical calculations were done for bamboo mat boards. The same approach could be used for bamboo strip boards.

3.5.1 Theoretical approach

The transmission forces mechanism in the tested corner connection is shown in Figure 3-15. Six free body diagrams can be seen in this figure. The body diagram 1 is showing the whole structure with its respective external reaction forces and the applied load *F*. The horizontal sheet support is called *A* and the vertical sheet support is called *C*. The horizontal and vertical reactions are distinguished by the subscript *x* and *y* respectively. The joints between every element are called B1, B2, B3 and B4. The rest of the diagrams show each of the elements (two plybamboo sheets, two 75x50 mm wood pieces and the 75x75 mm piece) separately. In appendix D, the calculation of the capacities of each of the joints is presented. Table 3-3 summarizes the results.

Table 3-3 Joint capacities for the corner connection.

Joint	Shear (N)		Withdrawal (N)		Yielding moment (Nmm)		Maximum moment (Nmm)	
	Nailed	Screwed	Nailed	Screwed	Nailed	Screwed	Nailed	Screwed
B1	1780	3980	1040	5720	17335	95335	26000	143000
B2	4440	-	2020	-	50475	-	75710	-
B3	2960	-	1345	-	33650	-	50475	-
B4	2670	5970	1560	8580	26000	143000	39000	214500

In appendix D the capacities are calculated per fastener. B1 and B3 are joined using two fasteners. B2 and B4 are joined using three fasteners. The values in Table 3-3 are obtained by multiplying the capacity per fastener by the number of fasteners in the joint.

From Figure 3-15, 18 equilibrium equations can be derived. These equations are as follows:

From free body diagram 1:

$$A_x = C_x \tag{3-2}$$

$$F = C_y + A_y \tag{3-3}$$

$$\sum M_A \Rightarrow 550F + 695C_x - 681C_y = 0 \tag{3-4}$$

From free body diagram 2:

$$B_{1x} = A_x \tag{3-5}$$

$$F = B_{1y} + A_y \tag{3-6}$$

$$\sum M_A \Rightarrow 550F - B_{1y}(600 - x_1) = M_{B1} \tag{3-7}$$

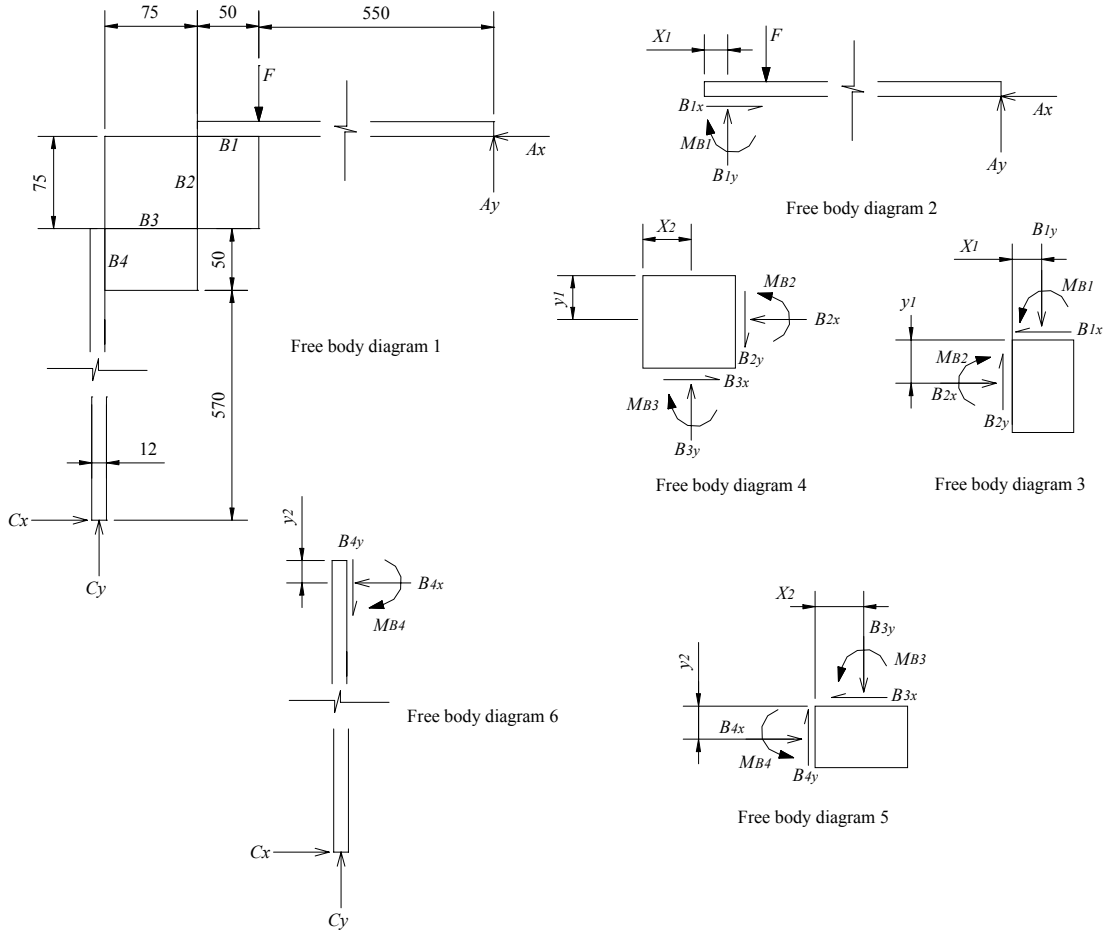

Figure 3-15 Free body diagrams of each of the corner elements (see notation in page iii).

From free body diagram 3:

$$B_{1x} = B_{2x} \tag{3-8}$$

$$B_{1y} = B_{2y} \tag{3-9}$$

$$\sum M_{upperleftcorner} \Rightarrow B_{1y}x_1 + M_{B2} = B_{2x}y_1 + M_{B1} \tag{3-10}$$

From free body diagram 4:

$$B_{2x} = B_{3x} \quad \textbf{(3-11)}$$

$$B_{2y} = B_{3y} \quad \textbf{(3-12)}$$

$$\sum M_{bottomrightcorner} \Rightarrow B_{3y}(75 - x_2) + M_{B3} = B_{2x}(75 - y_1) + M_{B2} \quad \textbf{(3-13)}$$

From free body diagram 5:

$$B_{3x} = B_{4x} \quad \textbf{(3-14)}$$

$$B_{3y} = B_{4y} \quad \textbf{(3-15)}$$

$$\sum M_{upperleftcorner} \Rightarrow B_{3y}x_2 = M_{B3} + M_{B4} + B_{4x}y_2 \quad \textbf{(3-16)}$$

From free body diagram 6:

$$B_{4x} = C_x \quad \textbf{(3-17)}$$

$$B_{4y} = C_y \quad \textbf{(3-18)}$$

$$\sum M_c \Rightarrow B_{4x}(620 - y_2) = M_{B4} + 6B_{4y} \quad \textbf{(3-19)}$$

In order to solve the equations system, six unknowns have to be supposed[3]. In general, the values x_1, x_2, y_1 and y_2 can be supposed with certain grade of accuracy because their ranges are known and are as follows (see Figure 3-15):
$0 \le x_1 \le 50$, $0 \le x_2 \le 75$, $0 \le y_1 \le 75$ and $0 \le y_2 \le 50$.

3.5.2 Theoretical calculations

3.5.2.1 Nailed connection

Figure 3-8 shows that there is a simultaneous failure in B1 and B4. From equations 3-4, 3-7, 3-19 and the horizontal sum of forces equations, the following expressions can be obtained:

$$F = \frac{1}{550}\left(\frac{-418050M_{B1} + 695x_1M_{B4} - 41700M_{B4} + 681M_{B1}y_2}{-46050 + 81y_2 - 620x_1 + x_1y_2}\right) \quad \textbf{(3-20)}$$

$$A_x = -1\left(\frac{6M_{B1} + x_1M_{B4} + 81M_{B4}}{-46050 + 81y_2 - 620x_1 + x_1y_2}\right) \quad \textbf{(3-21)}$$

[3] There are 15 independent equations and 21 unknowns including F.

$$C_y = \left(\frac{-620M_{B1} + M_{B1}y_2 - 695M_{B4}}{-46050 + 81y_2 - 620x_1 + x_1y_2} \right) \quad \textbf{(3-22)}$$

It can be assumed that the yielding moments in B1 and B4 are 17335 and 26000 Nmm respectively (see Table 3-3). These failures are caused by the withdrawal of the nails in B1 and B4 and soon the structure becomes a mechanism. x_1 and y_2 can be assumed as 8.33 and 41.7 mm respectively considering that the reaction forces B_{1y} and B_{x3} are located at two thirds from the neutral axis (see body diagrams 2 and 5 in Figure 3-15 and Figure D-2 from appendix D). Since no failure in B2 or B3 occurs, x_2 and y_1 are taken as 37.5 mm (see body diagrams 3 and 5 in Figure 3-15). With the previous values, the following results are obtained:

F = 668 N, C_y = 592 N, A_x = 51 N, M_{B2} = 14320 Nmm and M_{B3} = -5945 Nmm.

Positive signs indicate that the force or moment direction is as shown in Figure 3-15 and negative signs indicate that the force or moment acts in the opposite direction than the one shown in Figure 3-15.

3.5.2.2 Screwed connection

The difference in the analysis of the screwed connection is that besides the failure in B1 and B4 there is a failure in B2 as well (see Figure 3-14).
When using equations 3-20, 3-21 and 3-22 with M_{B1} = 95335 Nmm, M_{B4} = 143000 Nmm and the same values for x_1, x_2, y_1 and y_2, the following results are obtained:

F = 3675 N, C_y = 3255 N, A_x = 280 N, M_{B2} = 78770 Nmm and M_{B3} = -32705 Nmm.

In this case, the calculated moment at B2 is larger than the calculated capacity (50475 Nmm, see Table 3-3). This could mean that the failure in B2 occurs first than that one in B1.

Assuming that there is a simultaneous failure in B2 and B4 and using equations 3-4, 3-7, 3-10, 3-19 and the horizontal sum of equations the following expressions can be found:

$$F = \frac{1}{550}\left(\frac{-139000M_{B4} - 139350M_{B2} + 227y_2M_{B2} + 227M_{B4}y_1}{-2y_1 - 15350 + 27y_2} \right) \quad \textbf{(3-23)}$$

$$A_x = -1\left(\frac{27M_{B4} + 2M_{B2}}{-2y_1 - 15350 + 27y_2} \right) \quad \textbf{(3-24)}$$

$$C_y = \frac{1}{3}\left(\frac{-695M_{B4} - 620M_{B2} + y_2M_{B2} + M_{B4}y_1}{-2y_1 - 15350 + 27y_2} \right) \quad \textbf{(3-25)}$$

When introducing M_{B2} = 50475 Nmm, M_{B4} = 143000 Nmm, x_1 = 25 mm, x_2 = 37.5 mm, y_1 = 12.5 mm (two thirds from neutral axis) and y_2 = 41.7 mm, the following results are obtained:

F = 3320 N, C_y = 2965 N, A_x = 278 N, M_{B1} = 121150 Nmm and M_{B3} = -43371 Nmm.

Here, the calculated moments at B1 and B3 are larger than the calculated capacities. However, when changing x_1 to 16 mm and x_2 to 41 mm, M_{B1} becomes 94455 Nmm and M_{B3} changes to 32990 Nmm. Both values are close to the calculated capacities (see Table 3-3).

3.5.3 Comparison between theoretical and experimental results

In the nailed connection, the theoretical failure load was 592 N whereas the experimental failure load was 512 N. This could be seen as a good approximation but more experimental tests would be needed to corroborate the magnitude of this load. Wooden materials have natural variability and important deviations from the mean values could also be expected. In the theoretical calculation, the ratio between C_y and F is about 89% whilst in the experimental result the derived value was 69%. However, in loading step 3 (Table 3-1 and Figure 3-6) the plate weight registered by the load cell was 90% of the real weight which coincide with the theoretical ratio. Moreover, the initial weights (specimen, loading plate, jack cylinder) are about 50% of the failure load so that the actual loading of the compression machine is reduced to a range of only 250 N.

In the screwed connection, the theoretical failure load is between 2965 and 3255 N depending on which failure mode is taken into account. The experimental yielding loads for mat boards were 1700, 3050 and 3400 N (see Table 3-2). Here, the variability is clear. The theoretical ratio between C_y and F is about 88% whereas in the experimental results the calculated value was about 80%. The load cell registered the same 90% of the real weight of the loading plate. The difference in the forces ratio could be due to the following factors:

1. The accuracy of the load cell (10 kN) is different from the accuracy of the compression machine (100 kN).
2. The loading jack could introduce horizontal forces which can affect the distribution of the loads and internal forces in the connection. It has to be noticed that the difference from 80 to 90% is just a difference in the horizontal reactions of about 50 N.
3. The connection in A could be transmitting bending moments due to the friction between the steel roller and the steel plate.

Additional remark:

It could be clearly seen that there were horizontal reactions due to the bending of the vertical sheet. A ratio of 80% would say that the horizontal reactions are approximately zero.

3.6 Conclusions

The capacity of the connection 1 in Figure 3-1 is given by the withdrawal capacity of the 2.8 mm nails. This withdrawal capacity cannot withstand high bending moments and a mechanism is created soon. Hence, it is not recommended to rely on such connection.

It can be calculated that the required load per nail in a corner connection is about 0.140 kN (1.1x0.625x2.5/12) considering a wind load of 1.1 kN/m^2. From the experimental results, the capacity per nail would be approximately 170 N which is 1.2 times the required capacity. It appears then that the connection would resist the required load. The previous is not correct because of the variability of the experimental test and the instability presented by the connection during the tests. The connection may resist the first hurricane but it will be weakened for the next one since the nails are withdrawn quite easy. Tests on full-scale corner connections would be necessary to see whether the withdrawal effect is present or not.

The use of glue (in addition to the nails) or screws instead of nails would increase approximately 6 times the capacity of the corner connection. However, the failure in the screwed connection is more ductile[2] than that one with glue. In general, both connections could be safely used.

The corner connection with bamboo strip boards (with ultimate loads of 3.8, 3.95 and 4.3 kN) is stronger and stiffer than that one with bamboo strip boards (with ultimate loads of 2.6, 3.4 and 3.6 kN).

The results of these tests would be of great help when designing and calculating full-scale tests.

4 T-CONNECTION

4.1 Introduction

This chapter deals with experimental tests for T-connections in the house design method. There are three possible T-connections as shown in Figure 4-1.
T-connection 1 (T1) would be used in external walls (2 external walls and one internal wall). T-connection 2 (T2) could be used in external and internal walls (three internal walls) and T-connection 3 (T3) would be needed for internal walls (see Figure B-1 in Appendix B). The chapter concentrates on T1 being the connection between three panels in an external wall.

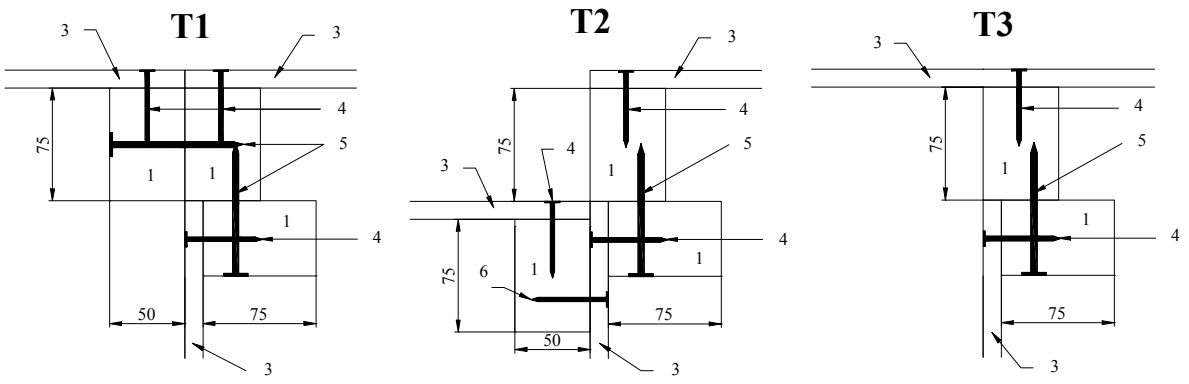

1. 75x50 mm wood piece
3. Plybamboo sheet (12 or 18 mm thick)
4. Screw (4.9 mm diameter, 50 mm long)
5. Nail (4.1 mm diamter, 88 mm long)
6. Nail (2.8 mm diameter, 55 mm long)

Figure 4-1 Top view of possible T-connections in design method A.

The purpose of the tests is to obtain the structural capacity of the T-connection. Knowing the capacity, design of such connections to withstand wind loads and earthquakes could be possible.
In order to analyze the structural behavior of this connection, part of the whole connection is modeled (see Figure 4-2). The same approach used for the corner connection is adopted.
The horizontal wind and seismic forces are modeled as a resultant force acting along the horizontal member of the model. In this case, two forces are acting on each panel. The two dimensional model is also shown in Figure 4-2.
After these considerations, the T-connection model was built and tested.
The test setup is described in section 4.2. Details of the construction of the model are also shown (section 4.2.1). This includes how the specimen was put together and mounted on a steel frame. In section 4.2.2 the loading procedure and deformation measurement system is explained.

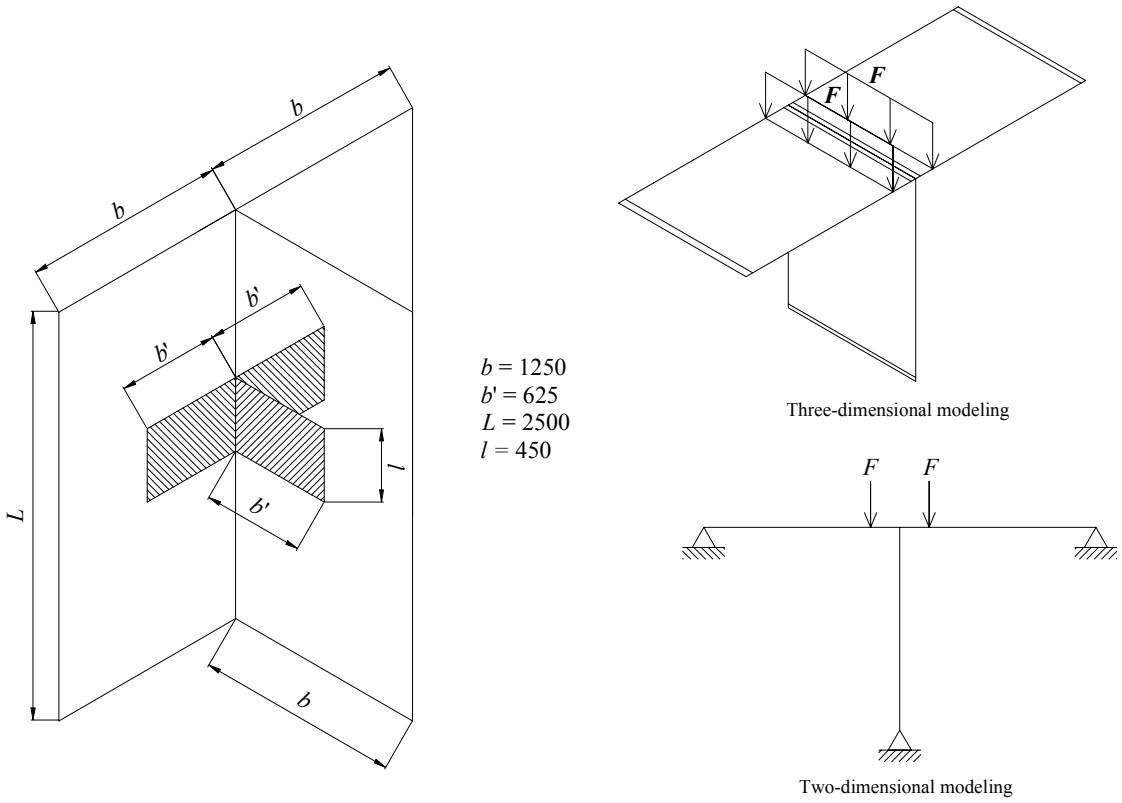

Figure 4-2 T-connection showing the part to be modeled, the three and two dimensional model.

The test series are presented in section 4.3. Three tests were performed using bamboo mat boards and three using bamboo strip boards. An additional test with an alternate design was also carried out (MB2). Experimental results and analysis are included in the section.
To complement the experimental results, a theoretical explanation of the structural behavior of the T-connection is presented in section 4.4. The analysis is based on theoretical capacities of the joints and the buckling capacity[4] of the sheets.
Finally, conclusions are given in section 4.5.

[4] Capacity required to avoid buckling.

4.2 Experimental setup

The steel frame used for the corner connection tests was modified in order to fixate the model for the T-connection. The frame offers an independent fixed reference system for measurement of displacements as well.

4.2.1 Specimen and frame

Figure 4-3 and Figure 4-4 shows how the specimen and steel frame were built. The specimen consists of three plybamboo sheets of 12(18)x625x450 mm (3) and three wooden pieces of 75x50x450 mm (1). The specimen is joined together as shown in detail 3 of Figure 4-4.

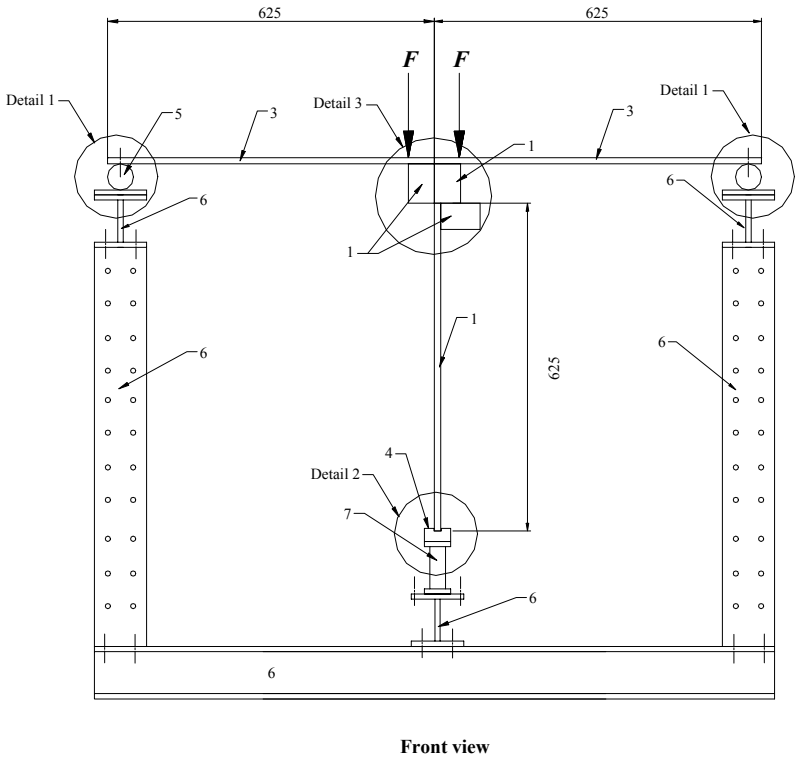

Figure 4-3 Test setup showing specimen and frame. For side view see figure 3.3.

Elements 1 and 3 represent the prefabricated panels which are joined together. In this case, three panels are joined to form the T-connection. The used wood is the same as the one used for the corner connection (K24 class B, see section 3.2.1).
The supports for the horizontal sheets and the vertical sheets (details 1 and 2) are the same as the ones used for the corner connection (see section 3.2.1 and Figure 3-4).
The steel frame is composed by wide flange H-beams (6).

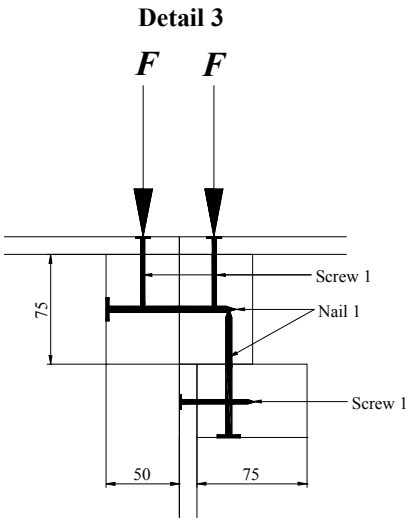

Nail 1: 4.1 mm diameter, 88 mm long.
Screw 1: 4.9 mm diameter, 50 mm long.

Figure 4-4 Detail 3 of Figure 4-3.

4.2.2 Measurement of load and deflection

As for the corner connection, two hydraulic jacks and a load cell were used to measure loads (Figure 4-5). The loading system was the same as the one used for the corner connection (see section 3.2.2). The loading procedure was simpler than the corner one because the initial loads could be disregarded due to the strength of the connection. Hence, the measurement of deflections was started at step 5 of Table 3-1.

The deflection measurement system consists of 3 digital dial gages placed on different positions in the specimen. Figure 4-6a shows a scheme in which each dial gage is numbered and Figure 4-6b shows a photograph of the actual test setup. Dial 0 measures the horizontal displacement at the center of the vertical sheet. 1 and 2 measure the vertical displacement of the 75x50 mm wood pieces.

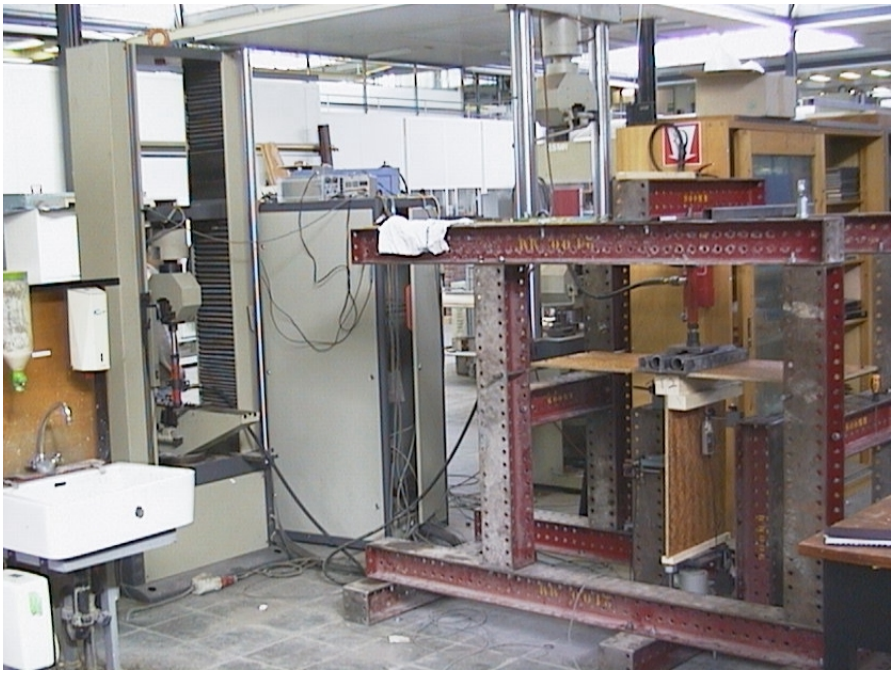

Figure 4-5 Experimental setup showing loading system.

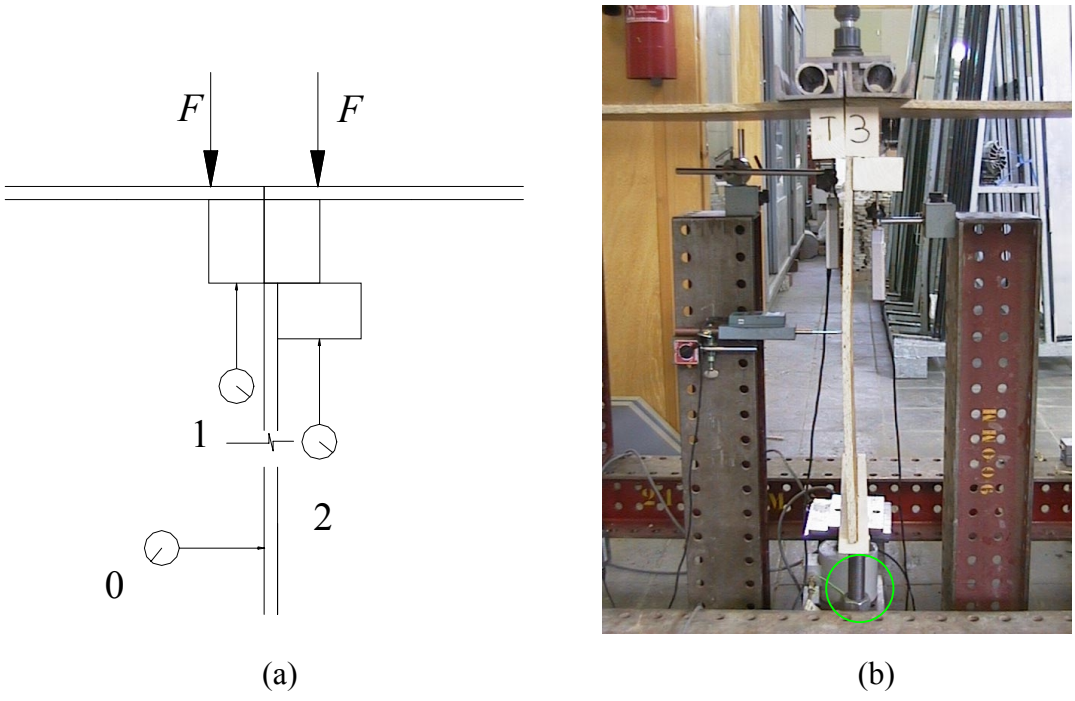

Figure 4-6 (a) Deflection measurement system scheme. (b) Test setup showing the deflection measurement system.

4.3 Test series and analysis

For the T-connection, seven tests were performed. 3 tests were done using bamboo mat boards (MB) and 3 using bamboo strip boards (SB) and an extra test (MB2) with a different design.
Table 4-1 shows a summary of the most important results for each of the tests.

Table 4-1 Test series results for the T-connection.

Test	$2F_y$ (kN)	$2F_u$ (kN)	δ_{0y} (mm)	δ_{1y} (mm)	δ_{2y} (mm)	F_{LC} / F_{CM}
MB1	8.43	16.1	0.19	2.65	2.17	0.916
MB3	7.53	15.3	0.71	2.63	2.10	0.932
MB4	7.82	12.5	0.93	3.09	2.52	0.933
SB1	16.0	16.0	0.76	4.29	2.64	0.928
SB2	14.0	14.0	1.42	5.81	2.71	0.920
SB3	20.0	20.0	3.32	4.53	2.92	0.931
MB2*	4.46	13.0	2.24	1.09	1.41	0.919

* Alternative design.

In Table 4-1, six results for each of the tests are shown (see also Figure 3-12):

1. $2F_y$ indicates the first decrease in the rigidity of the connection.
2. $2F_u$ is the ultimate load or maximum load registered by the compression machine.
3. δ_{0y} is the horizontal deflection (at the center of the vertical sheet) read at $2F_y$. See dial gage 0 in Figure 4-6.
4. δ_{1y} is the vertical deflection of the middle point of the 75x50 mm wood piece located to the left (see Figure 4-6).
5. δ_{2y} is the vertical deflection of the middle point of the 75x50 mm wood piece located to the right (see Figure 4-6).
6. F_{LC} is the force measured by the load cell whereas F_{CM} is the force measured by the compression machine. The previous was done by comparing the increase of the two forces in the same period of time. This time was taken in the straight part of the load-deflection curves.

4.3.1 Test MB1, MB3 and MB4

Test MB1:

At the beginning of the test, the vertical sheet was moving slightly to the left (in Figure 4-10, a movement to the left is positive and a movement to the right is negative). Afterwards, it moved to the right. This effect can be seen in the black curve of Figure 4-10a. At around 8.4 kN, the sheet is finally moving to the left. Beyond this load, the rigidity decreased until the ultimate load of 16 kN was reached. This was the strongest and stiffest connection of the bamboo mat boards.
The vertical movement of point 1 (Figure 4-6) is also shown in Figure 4-10b. It can also be seen that the rigidity starts to decrease at 8.4 kN when the displacement is 2.65 mm.

Test MB3:

This test shows a similar behavior than test MB1 but less rigid and less strong (see yellow curve in Figure 4-10).

Test MB4:

This test showed a different behavior than tests MB1 and MB3. The reason is that the vertical sheet began to move immediately to the left which makes the connection less rigid (see turquoise curve in Figure 4-10). However, this connection was more rigid than MB2. The failure load was 12.5 kN which is the lowest of the four tests made on the bamboo mat boards.

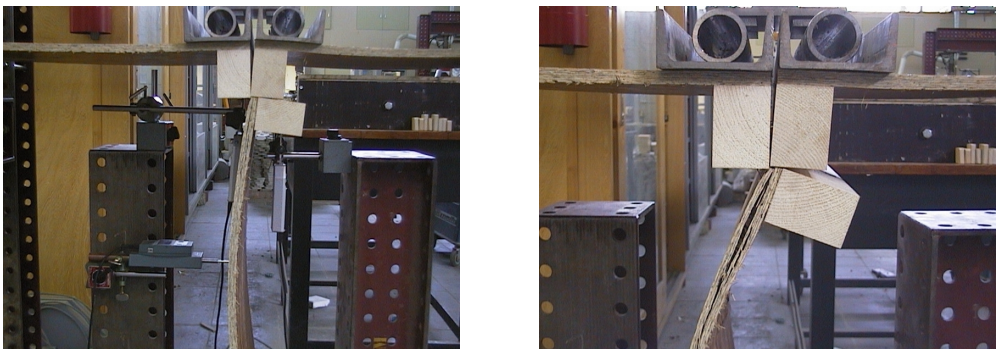

(a) (b)

Figure 4-7 (a) MB1 test showing failure mode. (b) MB1 test showing failure in the vertical sheet.

4.3.2 Test SB1, SB2 and SB3

The failure mode of the connections using bamboo strip boards is given by the bending of the nails that join the two horizontal panels (Figure 4-8b). This is due to the fact that the strip boards are thicker and stiffer than the mat boards. Hence, the buckling capacity is higher than the nailed joint. In Table 4-1, the values for $2F_y$ and $2F_u$ are the same because the tests were stopped when the deflection δ_{ly} was approximately 5 mm. The deflection values represent the maximum values registered during the test.

(a) (b)

Figure 4-8 (a) SB1 test showing failure mode. (b) 75x50 wood piece removed from the left panel after the test showing how the nails were bent.

4.3.3 Test MB2

There was a change in the design of this T-joint in order to compare the behavior with the other tests. The vertical sheet is placed below the left panel as shown in Figure 4-9. The experiment showed that the vertical sheet starts bending immediately to the left and is less rigid than the original design. The rigidity of the connection starts decreasing at 4.5 kN (see pink curve in Figure 4-10) with a horizontal deflection of 2.2 mm. The rigidity is completely lost at 11 kN but the sheet is still deforming until a maximum load of 13 kN. It can be seen in Figure 4-10b that the vertical movement of point 1 requires more load to reach the same deflection. This is due to the fact that the wood piece on the left panel is in direct contact with the vertical sheet.

Figure 4-9 MB2 test showing failure mode.

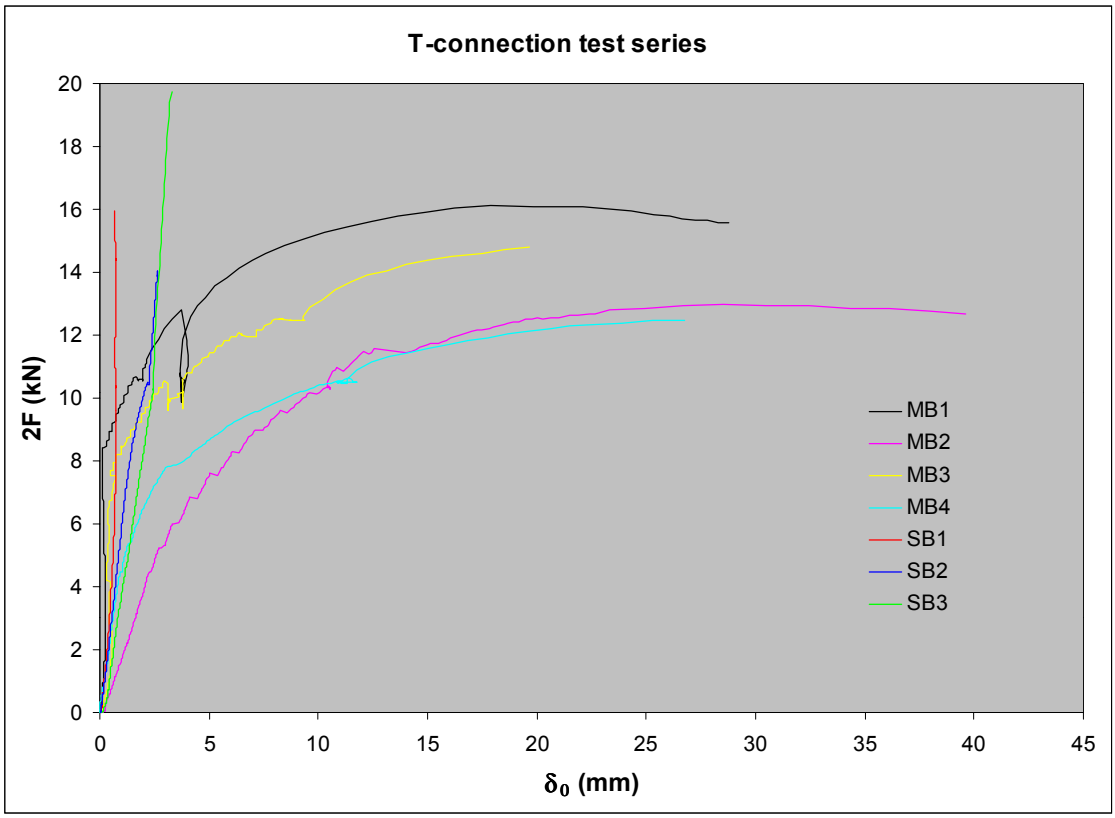

(a)

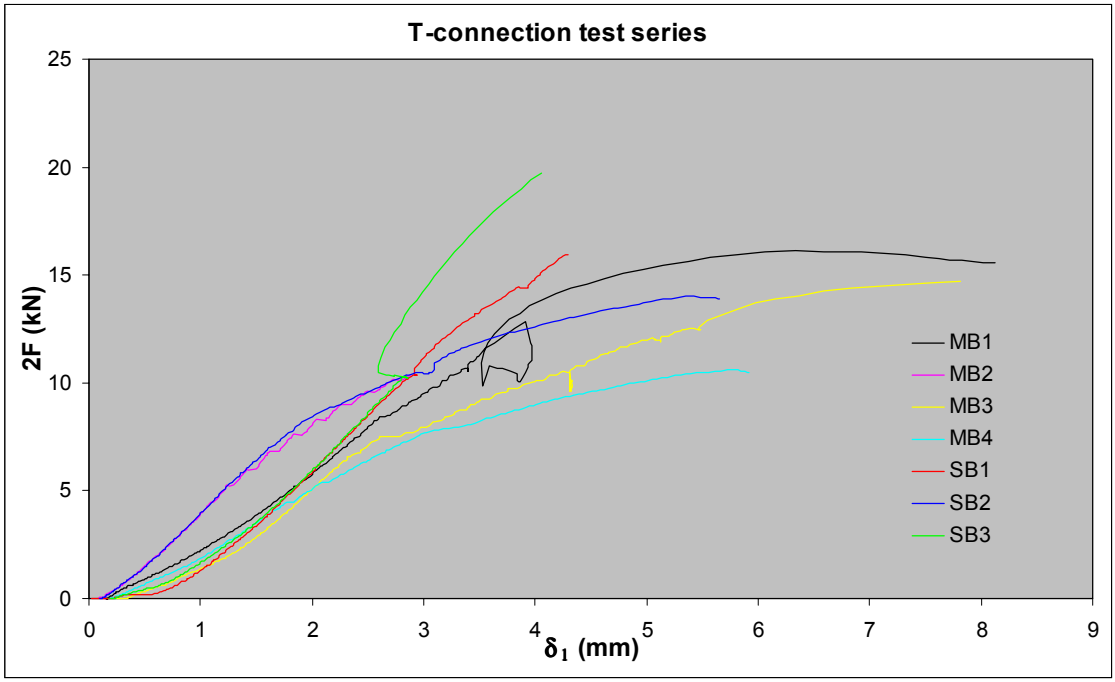

(b)

Figure 4-10 (a) Load-deflection curves for displacement 0. (b) Load-deflection curves for displacement 1.

The alterations in the curves at about 10 kN are due to the fact that the load cell in the bottom had a capacity of 10 kN. At this time, two bolts were also holding the specimen (see green circle in Figure 4-6b).

4.4 Structural behavior according to the experimental results

Figure 4-11 shows a free body diagram of the T-connection used in the experiments. As can be seen in table 4.1, the reaction force at the bottom is 92.5% of *2F* in average which means that $F_1 = 0.925F$. In theory, the distance *d* from the load *F* to the point where the resultant load F_1 is transmitted can be calculated (see Figure 4-12). From Figure 4-12,

$$\sum M_1 \Rightarrow 550F = F_1(550 + d) \qquad \textbf{(4-1)}$$

Substituting $F_1 = 0.925F$ in equation (4-1) a value of $d = 44.6$ mm is obtained. It can be concluded from this value that the force F_1 on the left is transmitted directly through the shear plane *A* in Figure 4-11 without the introduction of important bending moments. The force F_1 on the right is transmitted through plane C.

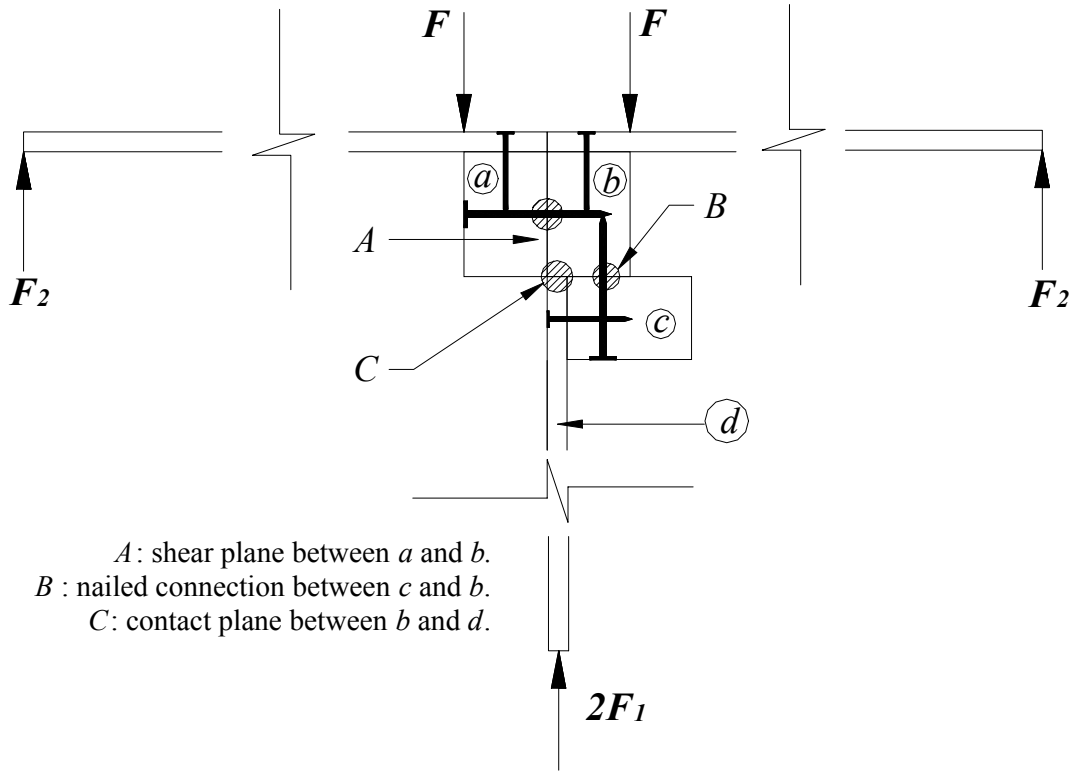

Figure 4-11 Free body diagram for the T-connection.

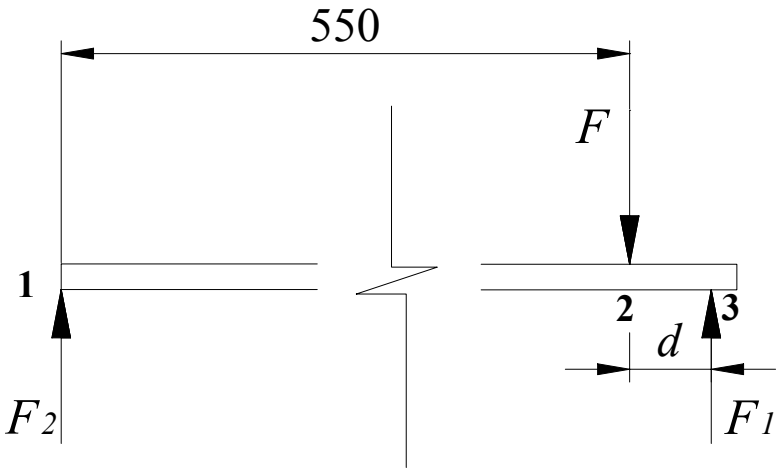

Figure 4-12 Free body diagram of the left horizontal sheet.

The capacity of shear plane *A* in Figure 4.11 is calculated in section D.1.1 of appendix D as 1479 N per nail. Three nails were used in the tests which means that the theoretical capacity of shear plane *A* is 4.4 kN. When the force transmitted by shear plane *A* is 4.4 kN, the force in the vertical sheet $2F_1$ is 8.8 kN.
The theoretical buckling capacity of the vertical sheet can be calculated with Euler's formula:

$$P_{cr} = \frac{\pi^2 EI}{L_{ef}^{\ 2}} \qquad \textbf{(4-2)}$$

The second moment of area of the vertical sheet using mat boards would be $I = t^3 b / 12 = 12^3 \text{x} 450 / 12 = 64800$ mm^4 whereas for strip boards would be $I = 18.6^3 \text{x} 450 / 12 = 241307$ mm^4. The bending modulus of elasticity of mat boards is $E = 3000$ N/mm^2 and of strip boards $E = 6500$ N/mm^2 (see Table A-1, page 60). The effective length L_{ef} could be assumed as 625 mm. With the previous values it can be found that:

$$P_{cr} = \frac{\pi^2 3000x64800}{625^2} = 4911\text{N} \text{ for mat boards and } P_{cr} = \frac{\pi^2 6500x241307}{625^2} = 39630\text{N}$$

for strip boards.

It is clear that the structural capacity of the T-connection using strip boards is given by the joint between *a* and *b* (see Figure 4-11) which is around 3.5 times less than the buckling capacity of *d*.
The obtained buckling capacity for the mat boards does not seem to fit with the experimental results. It can be noticed that the experimental capacities (14 kN in average) are 2.8 times higher than the theoretical value (4.9 kN). The previous could be due to three factors:

1. L_{ef} = 575 mm (625-50) instead of 625. For this case, P_{cr} = 5800 N.

2. $572/\sqrt{2} \le L_{ef} \le 575$ considering that there is moment capacity at the top connection of the vertical sheet. In the case that full-moment capacity is considered, $L_{ef} = 575/\sqrt{2} = 406\,\text{mm}$ and P_{cr} = 11600 N which is an upper limit.

3. The modulus of elasticity E_m = 3000 N/mm^2 is lower than E in equation 4-2. For instance, if $L_{ef} = \left(575 + 575/\sqrt{2}\right)/2 = 491$ mm and P_{cr} = 14000 N (which is the average value obtained in the tests) a value of E = 5280 N/mm^2 is found.

4.5 Conclusions

Considering a wind pressure of 1.1 kN/m^2, a 1.2 kN load (1.1x2.5x0.45) will be acting on the analyzed T-connection. The lowest experimental capacity was 12 kN which is 10 times the required one. It can be concluded then that the T-connection is the strongest link of the structural chain covered by the experiments.

The T-connection using strip boards is stronger than that one using mat boards because of the higher second moment of area I and modulus of elasticity E. Anyway, both connections can be safely used.

The differences between the experimental and theoretical values in the case of mat boards could be due to the orthotropic characteristics of the plybamboo. Tests on compression modulus of elasticity E_c could be carried out in order to calculate a new theoretical buckling capacity.

After having studied the behavior of the corner and T-connections, the next step would be to investigate the parallel connections. However, this is not as simple as the corner and T-connections because when the parallel connection is simplified into two dimensions, it becomes a mechanism (Figure 4-13). In reality, this will not occur because the vertical members transmit the forces to the lower and upper soleplate by bending (see section 2.3).

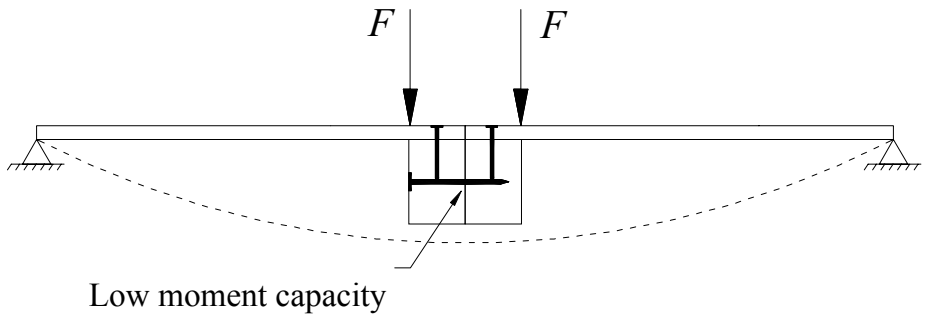

Figure 4-13 Parallel connection being analyzed as a two-dimensional structure.

5 SHEET TO FRAME CONNECTION UNDER LATERAL LOAD

5.1 Introduction

The next important connection for the walls would be the one between the frame and the sheet under lateral load (section 2.5). In section 2.5, a model was used to calculate the capacity of such connection. The purpose of the following tests is to compare the theoretical model [4] with the experimental results. For the experimental model, a plybamboo sheet of 1200x1200 mm was used (see Figure 5-2b).

The difference between the real panel (Figure 5-2a) and the experimental model depends on the bending moment M_1 or M_2 that is transmitted to the foundation. For the real panel, $M_1 = R_1 L = TL/2 \Rightarrow R_1 = T/2$ whereas in the experimental model, $M_2 = R_2 L/2 = TL/2 \Rightarrow R_2 = T$. From the previous, it could be derived that $R_2 = 2R_1$ which means that the resistance to lateral load of the experimental model is twice that one of the real panel considering that the tension T in both vertical members is the same.
The following section describes the experimental setup including specimen and frame and measurement of load and deflection. In section 5.3, the experimental results and its respective analyses are presented. Section 5.4 deals with the comparison between theoretical and experimental results and section 5.5 finishes the chapter with some conclusions.

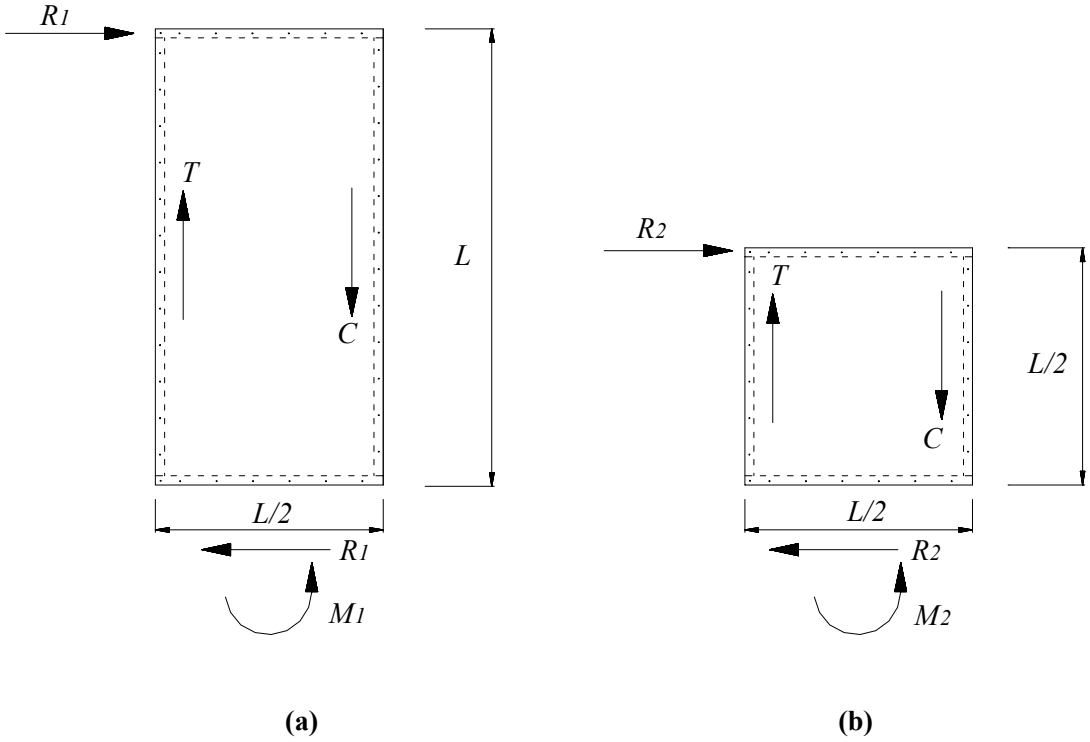

Figure 5-2 (a) Real prefabricated panel submitted to lateral load. (b) Experimental model for specimen submitted to lateral load.

5.2 Experimental setup

5.2.1 Specimen and frame

The test specimen consists of a plybamboo sheet joined to a wooden frame as shown in Figure 5-3. Screws spaced every 190 mm were used to join the vertical members to the sheet whereas nails were used to join the horizontal members and the sheet. In reality, the nailed joints would be carried out on site and the screwed joints would be made in factory.

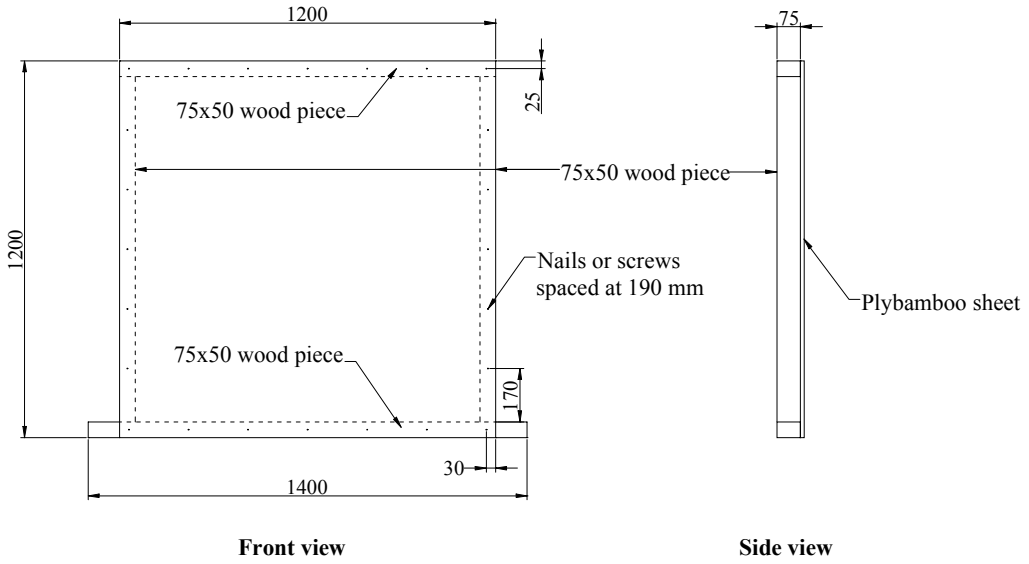

Figure 5-3 Test specimen.

The test specimen was mounted on a steel frame as shown in figure 5-4.

1. H-beam.
2. Steel bar.
3. Test specimen (Figure 5-3).
4. Hydraulic jack and load cell providing a tensile force.
5. Steel plate
6. Bolts

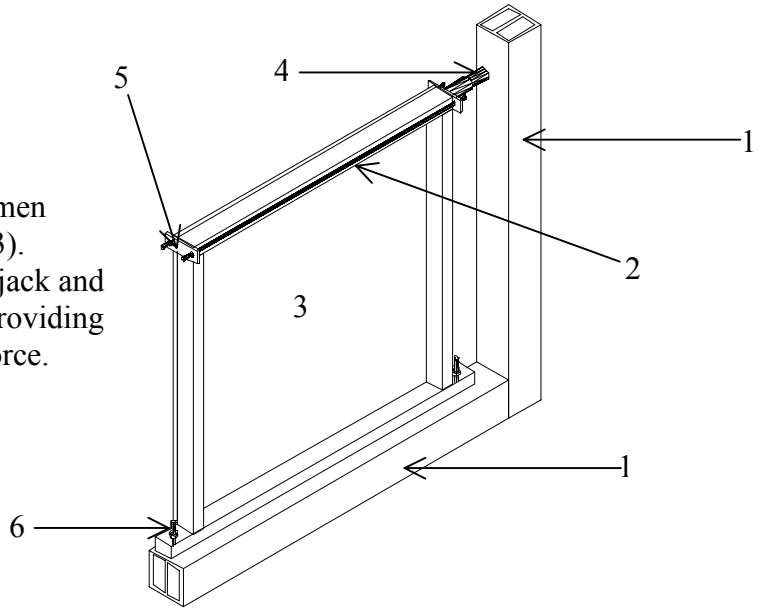

Figure 5-4 Test specimen mounted on the steel frame.

The steel frame consists of a corner formed by two H-beams (1). The test specimen (3) is joined to the horizontal H-beam using two bolts (6). Two steel bars (2) joined to steel plates (5) at each end are placed on the top of the specimen as shown in Figure 5-4. A hydraulic jack and a load cell (4) are joined to one of the steel plates (5) and the vertical H-beam (1). The idea is to produce a concentrated load in the center of the cross-section of the upper soleplate. When the jack starts to pull the plate, the steel bars are pulled as well and transmit the load to the plate on the other extreme producing the wanted load (see section 5.2.2 for more details). If the jack were pushing instead of pulling there would not be a free rotation of the panel where the load is applied because the jack would restrict this rotation.

5.2.2 Measurement of load and deflection

In order to apply a horizontal load as shown in the model of Figure 5-2, two steel bars were pulled by a hydraulic jack (yellow circle in Figure 5-5) which is fixed to a vertical H-beam producing a horizontal load on the other extreme transmitted from the steel bars to a steel plate (see Figure 5-6c). The load cell (green circle in Figure 5-5) is connected to a steel plate as shown in the yellow circle of Figure 5-6d and is in charge of measuring the load. The load is applied by a pneumatic pump (blue circle in Figure 5-5) at an approximate rate of 1 kN/min.

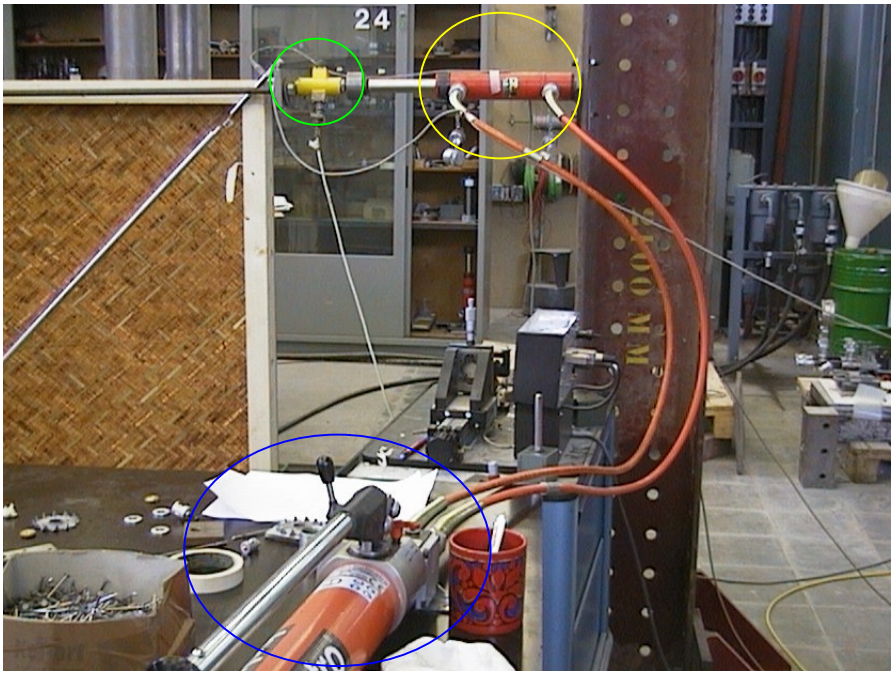

Figure 5-5 Measurement of load equipment.

The measurement deflection system consists of three different deformations:

1. Deformation of the wooden frame (D2frame, Figure 5-6a): a hollow aluminum tube was joined to the opposite corners of the wooden frame and a LVDT which can freely rotate (green circle in Figure 5-6d) measures the deformation of this diagonal.

2. Deformation of the plybamboo sheet (D1sheet, Figure 5-6b): the method is the same as the previous one.

3. Horizontal displacement (green circle in Figure 5-6b): a digital dial gage is placed in the middle of the horizontal member cross-section. This would measure the horizontal displacement at the point where the load is acting.

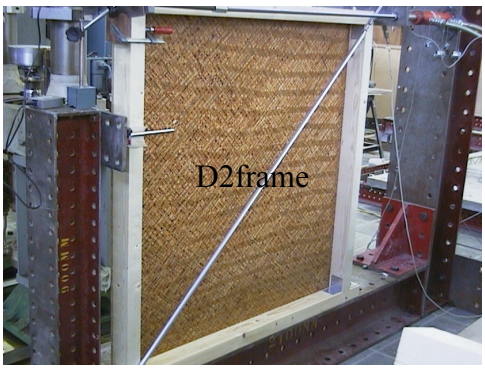

(a) Diagonal joined to the wooden frame.

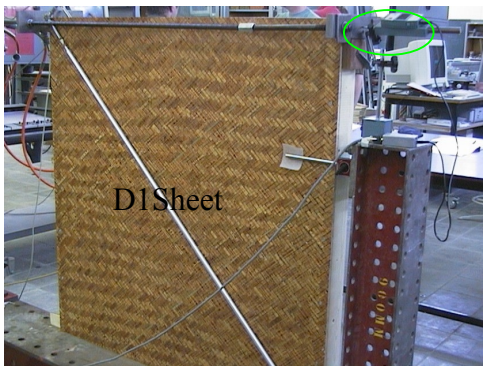

(b) Diagonal joined to the plybamboo sheet.

(c) Transmission of horizontal load through horizontal member.

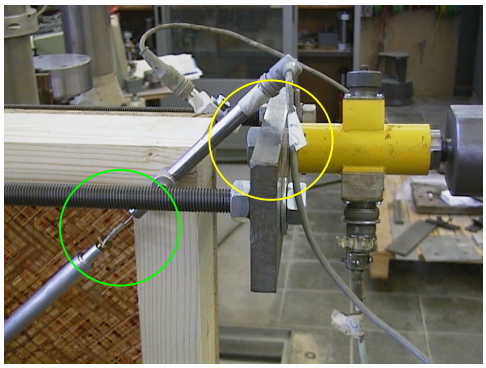

(d) LVDT and load cell detail.

Figure 5-6 Details of measurement of deflection and load.

5.3 Test series and analysis

Seven tests were made in total. The first four were done using bamboo mat boards whereas the other three were done using bamboo strip boards. Appendix E shows the experimental curves obtained from each of the tests and Table 5-1 presents the most significant results. Figure 5-7 schematically explains each of the results presented in Table 5-1. The deflections δ_y and δ_u in Table 5-1 and Figure 5-8 are the horizontal displacements of the point where the load is applied (see section 5.2.2).

Table 5.1 Experimental results for test series on lateral load.

Test	F_y (kN)	δ_y (mm)	δ_u (mm)	k (kN/mm)
MB1	1.8	3.3	8.9	0.54
MB2	5.4	10.2	25.2	0.53
MB3	4.4	7.1	28.3	0.62
MB4	5.4	9.3	26.4	0.58
SB1	4.7	11.5	28.1	0.41
SB2	4.1	7.1	17.8	0.58
SB3	4.6	10.2	18.3	0.45

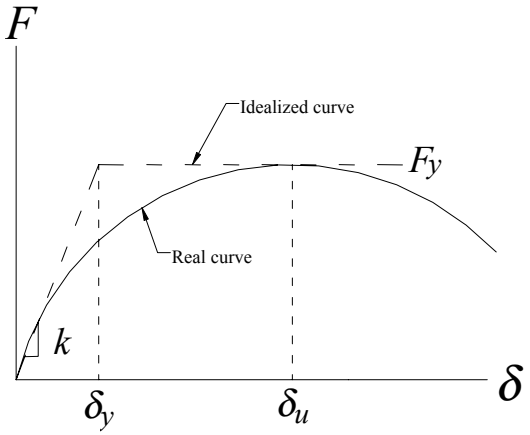

Figure 5-7 Load-deflection curve scheme under lateral load showing certain parameters.

5.3.1 Test MB1

The first test was made with bamboo mat board but the wooden frame was not joined in the corners. The capacity was 1.8 kN (see black curve in figure 5-8). The failure was due to the yielding of the nail in the corner (see Figure 5-9). See in figure E-1 of appendix E the deformation of the diagonal in the sheet (D1sheet), the diagonal of the frame (D2frame) and the horizontal displacement. The first one does not even reach one millimeter whereas the other two are in the same level of magnitude.

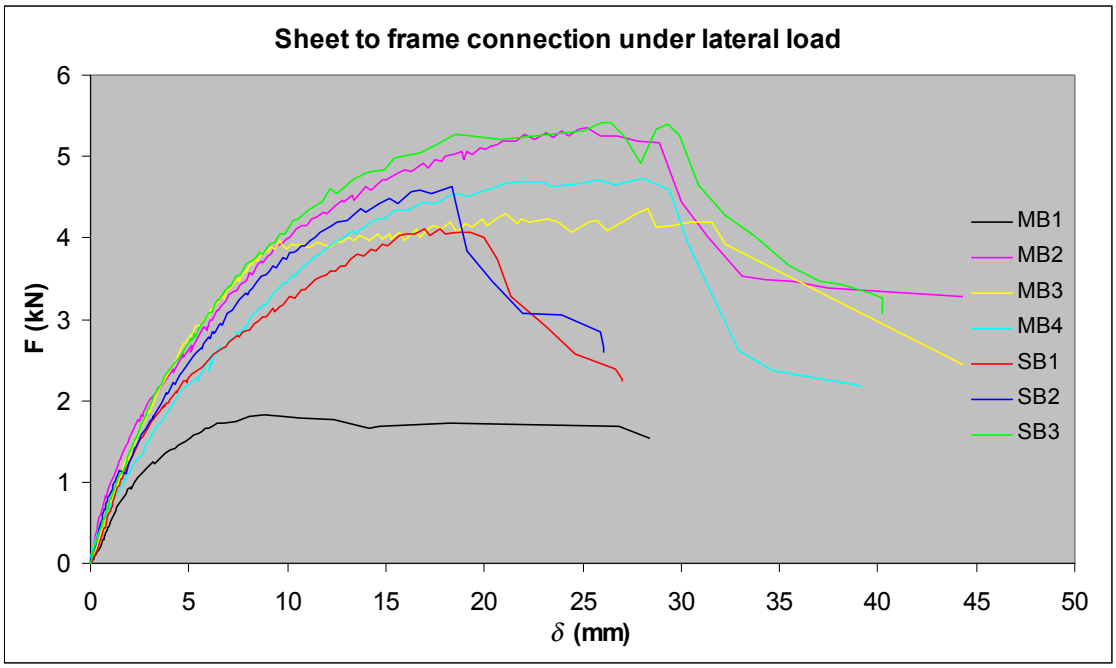

Figure 5-8 Load-deflection curves obtained from the experimental tests.

Figure 5-9 Failure in test MB1 due to the high deformation of the nail in the corner. The vertical member is not joined to the lower soleplate.

5.3.2 Test MB2, MB3 and MB4

As can be seen in Figure 5-8, tests MB2 and MB4 showed similar behaviors reaching an ultimate load of 5.4 kN. Test MB3 seemed to be more rigid at the beginning but reached its failure load at 4.4 kN. The structural behavior could be summarized in three phases (see Figure 5-7):

1. At the beginning, the structure deforms at certain rigidity *k* given by the connection of the sheet and the frame.
2. When the nail in the corner (Figure 5-9) is yielding (the vertical load component in the nail seems to be higher than the horizontal component), the angular steel plate starts to yield and the rigidity *k* decreases.
3. Finally, the screws joining the vertical member and the lower soleplate are withdrawn causing the failure of the structure (see Figure 5-10).

Figure 5-10 Ultimate failure in connection between the vertical member and the lower soleplate using mat boards.

5.3.3 Tests SB1, SB2 and SB3

The experimental tests using strip boards showed a similar behavior than those ones using mat boards. Tests SB1 and SB3 reached about the same ultimate capacity (4.7 and 4.6 kN respectively) but the load in SB3 started to decrease at a lower deflection. Test SB2 were the weakest one with an ultimate load of 4.1 kN and a decrease in the load similar to SB3. The typical failure previously explained can be observed once more in Figure 5-11.

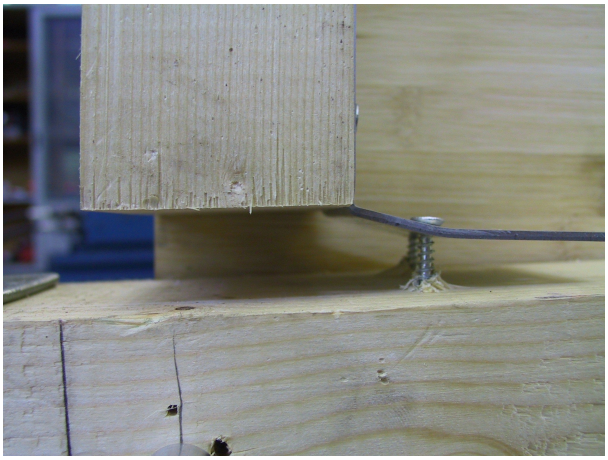

Figure 5-11 Ultimate failure in connection between the vertical member and the lower soleplate using strip boards.

5.4 Structural behavior according to the experimental results

This section deals with theoretical calculations obtained from known models and the comparison between these ones and the experimental results.
In order to calculate the resistance of the sheet to frame connection under lateral load, the model of equations 2-7, 2-8 and 2-9 (Figure 5-12) is used. With this model, the following procedure for the experimental specimen is applied:

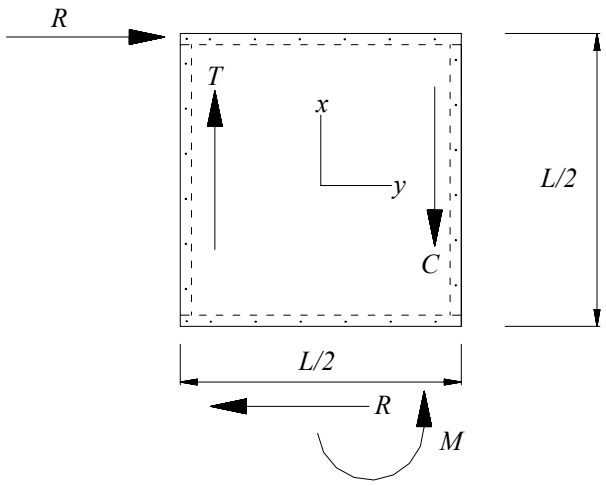

Figure 5-12 Structural model of the experimental specimen.

$$\sum x_i^2 = 7x2x575^2 + 4\left(190^2 + 380^2 + 570^2\right) = 6.65x10^6\,\text{mm}^2,$$

$$\sum y_i^2 = \sum x_i^2 = 6.65x10^6\,\text{mm}^2,$$

$$F_{x,i} = \frac{1200x575R}{6.65x10^6} = 0.104R\,,\ F_{y,i} = F_{x,i} = 0.104R\,,$$

$$F_i = \sqrt{(0.104R)^2 + (0.104R)^2} = 0.147R \Rightarrow R = 6.8F_i$$

From section D.1.4, F_i = 891 N for mat boards, hence
R = 6.8x891 = 6059 N = 6.0 kN.
For strip boards, t_1 = 18.6 mm, t_2 = 55-18.6 = 36.4 and $f_{h,1}$ = 86 N/mm^2.
Repeating the procedure of section D.1.4, it can be found that F_i = 883 N
$\Rightarrow R = 6.8x883 = 6004$ N = 6.0 kN.

The previous model assumes that the vertical members are anchored to the foundation so that uplifting is prevented. In the experiment, the vertical members are joined to the lower soleplate which is bolted to the H-beam. In the test, the angular steel plate below the point where the load is applied yields until the screws are withdrawn causing the uplifting of the vertical member in tension (see Figure 5-10). The full capacity given by the sheet and the frame is not developed because of this phenomena.
Figure 5-13 shows the failure mechanism of the connection between the vertical member and the lower soleplate. At a tension force T_1, the panel is still in the elastic range (Figure 5.13a). When T_1 increases to T_2, the angular steel plate yields and the initial rigidity k commences to decrease (Figure 5.13b). Finally, when T_2 increases to

T_3 the screws joined to the lower soleplates are withdrawn and sometimes the screws joined to the vertical members are withdrawn as well (Figure 5.13c).

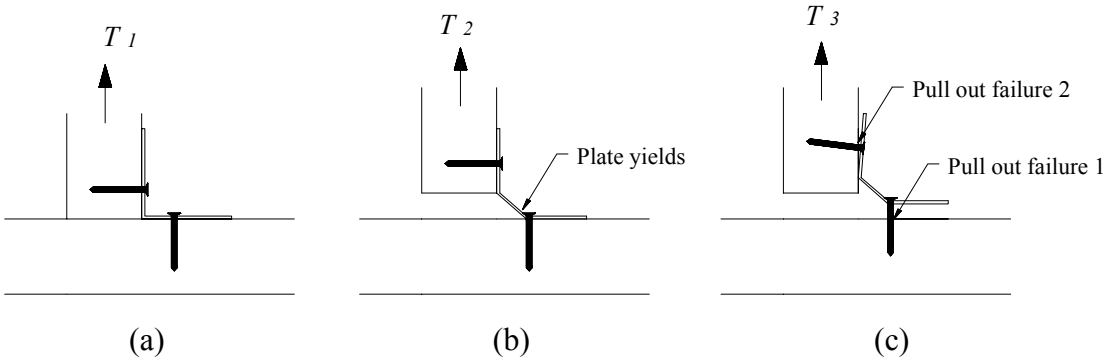

Figure 5-13 Failure mechanism of connection between vertical member and lower soleplate.

It was derived in section 5.1 that the lateral resistance R_2 of the experimental specimen would be equal to the tensional force produced in the vertical member (see Figure 5-2b). Hence, the lateral resistance is governed by the capacity of the connection shown in figure 5-13.

5.5 Conclusions

The experimental specimen showed in all cases a ductile behavior (capacity to deform without increasing the load) under lateral load which is adequate in case of seismic or wind loads.

The theoretical calculated capacity (6 kN) is higher than the experimental obtained capacity (4.8 kN in average) because the connection between the vertical member and the lower soleplate is not strong enough. Hence, this connection governs the structural capacity of the specimen.

In the case of the real panel (2500x1250 mm) the lateral load $R_1 = T / 2$ (see section 5.1) which means that the lateral resistance would be half of that one obtained in the actual tests. The best way to improve this is to use four screws instead of the two that were used for making this joint.

As concluded in chapter 2, the required 4.3 kN in each shear wall could be withstood by two complete (without windows nor door openings) panels. This must be corroborated by carrying out tests on full-scale walls under lateral load and with the real foundation to wall connection.

REFERENCES

1. IPIRTI (1999). Manufacture of Bamboo Mat Board, a manual. Project Bamboo Mat Board. India. 27p.

2. González, G.E. (2000). Determination of the embedding strength of plybamboo. Eindhoven University of Technology. Report CO-01-03. The Netherlands. 42p.

3. Szilard, R. (1974). Theory and analysis of plates. Classical and numerical methods. Prentice-Hall. United States of America.

4. Blass, H.J. et al (1995). Timber engineering-Step 1. First Edition, Centrum Hout, The Netherlands.

5. FUNBAMBU (1998). Bamboo Housing Technology Transfer Workshop. Costa Rican Bamboo Foundation. Guápiles, Costa Rica.

6. International Code Council (2000). International Building Code. United States of America, 756p.

7. Eurocode 5 (1993). Timber structures. Part 1-1: General rules and rules for buildings. European Committee for Standardization (CEN). English version. 110p.

8. González, G. et al (2001). Selection criteria for a house design method using plybamboo sheets. Journal of Bamboo and Rattan. INBAR. China. 12p.

APPENDICES

A. PLYBAMBOO PROPERTIES

Mechanical, physical and geometrical properties of plybamboo sheets

The following tabulated (Table A-1) values are mean, characteristic and design values for several properties of two kinds of plybamboo. These values are defined here and are used for theoretical calculations in experimental and structural design. Usually, the mean values are used for experimental calculations whilst design values are used for structural design. These values are not meant to be used for practical purposes. If engineers decide to build using these materials as structural elements in construction, tests must be carried out before implementing them in practice.

Notation to Table A-1

Mechanical properties:

f_m : bending strength.
f_t : tensile strength.
f_c : compressive strength.
f_v : shear strength.
f_h : embedding strength.
E_m : bending modulus of elasticity.

All these mechanical properties are given in N/mm^2.

Physical properties:

ρ : density at standard room temperature (20ºC $\pm$ 2) and humidity (65% $\pm$ 5) in kg/m^3.
$\%w$: moisture content at standard room temperature and humidity in percentage.

Subscripts:

mean : mean value.
k : characteristic value.
d : design value.
0 : parallel to the grain.
90 : perpendicular to the grain.

Notes:

- Usually a design value is the characteristic value multiplied by the following factor: $\frac{1.1}{1.3} = 0.846$,where 1.1 is the k_{mod} (factor that takes into account the duration of the load given in table 3.1.7 of reference 7) for instantaneous loads like earthquakes and hurricanes and 1.3 is the material safety property γ_M used for wood and wood-based materials (table 2.3.3.2 of reference 7).

- The characteristic value is defined as the lower 5-percentile value obtained from the experimental data. This value is calculated with the following formula:
  $f_k = f_{mean} - 1.56SD$, where f_k is the characteristic value of a mechanical property, f_{mean} is the mean value of a mechanical property and SD is the standard deviation obtained from tests.

- The mechanical characteristic values were obtained multiplying the mean values by 0.7 which means that the variation coefficient is around 0.2 or 20%. In the case of f_h, the values were obtained by the author from experimental results [2].

- The mean values for MB were taken from reference 1 except f_h [2] and f_v which was taken as a regular value for plywood whereas mean values for SB were provided by Mr. Samuel Yao from Qinfeng Bamboo Flooring (Internet address: http://www.china-qingfeng.com).

Table A-1 Several plybamboo properties to be used in this report

Property / Type of plybamboo	MB	SB
$f_{m,mean}$	60	94
$f_{m,k}$	42	66
$f_{m,d}$	36	56
$f_{t,0,mean}$	30	105
$f_{t,0,k}$	21	74
$f_{t,0,d}$	18	63
$f_{c,0,mean}$	35	52
$f_{c,0,k}$	25	36
$f_{c,0,d}$	21	30
$f_{c,90,mean}$	-	18
$f_{c,90,k}$	-	13
$f_{c,90,d}$	-	11
$f_{v,mean}$	5	9
$f_{v,k}$	3.5	6
$f_{v,d}$	3	5
$f_{h,mean}$	92	86
$f_{h,k}$	80	74
$f_{h,d}$	68	63
$E_{m,mean}$	3000	6500
$E_{m,k}$	2100	4550
ρ_{mean}	790	720
$\%\, w$	-	8-10
t_{mean}	12	18.6
L_{mean}	2500	2500
b_{mean}	1250	1250

B. HOUSE DESIGN EXAMPLE

This appendix shows an example of a house design using prefabricated walls made of plybamboo sheets and wood. Details of the floor plan, foundation and walls as well as wall to wall, wall to foundation and wall to roof connections are presented.

B.1 Floor plan

Figure B-1 shows a plan view of a possible house constructed with prefabricated panels. It also shows the modular basis of 1250 mm, the different types of joints between walls and the places in which the panels must have a window (**w**) or door opening.

B.2 Walls

The walls consist of prefabricated panels transported from the factory and then mounted on-site. Figure B-2 shows three different types of prefabricated walls regarding the building process and the structural design. Panel A consists of a plybamboo sheet (2500x1250x12 mm) joined to a wooden frame. In this case, the size of the frame coincides with the size of the sheet. The vertical and horizontal members are joined in the corners by angular steel plates as shown in Figure 2-4. Panel B consists of a smaller wooden frame than panel A. The idea is to cover the upper and lower soleplates (see section B.3 and B.4) with the plybamboo sheet. In this way, the soleplates would not be exposed to the outside. Besides, structural capacity to resist lateral load is improved (see section 2.6). However, more work on-site will be needed. The idea of panel C is to eliminate the horizontal members. In this case, the joint between the vertical members and the soleplates must be made on-site as well as the joint between the sheets and the soleplates. The previous would have an impact on the structural design of the upper soleplate (see section 2.5).

B.3 Foundation

The left part of Figure B-3 shows a vertical section of a possible wall to foundation connection based on the footing system that has been used by the Costa Rican Bamboo Foundation [5]. It consists of a reinforced concrete strip footing (this one might be another type depending on the place in which the method is being applied). Two conventional concrete hollow blocks (i.e.12x20x40 cm) are placed above the concrete strip. Steel bars coming from the footing are passed through the hollow part of the blocks. This part is afterwards filled with mortar. These blocks provide a barrier against humidity and termites. The lower soleplate is fixed to the concrete blocks by means of the steel bars coming from the foundation. This is achieved by passing the steel bars through predrilled holes in the soleplate over 10 cm and hammering them to anchor the lower soleplate to the blocks.

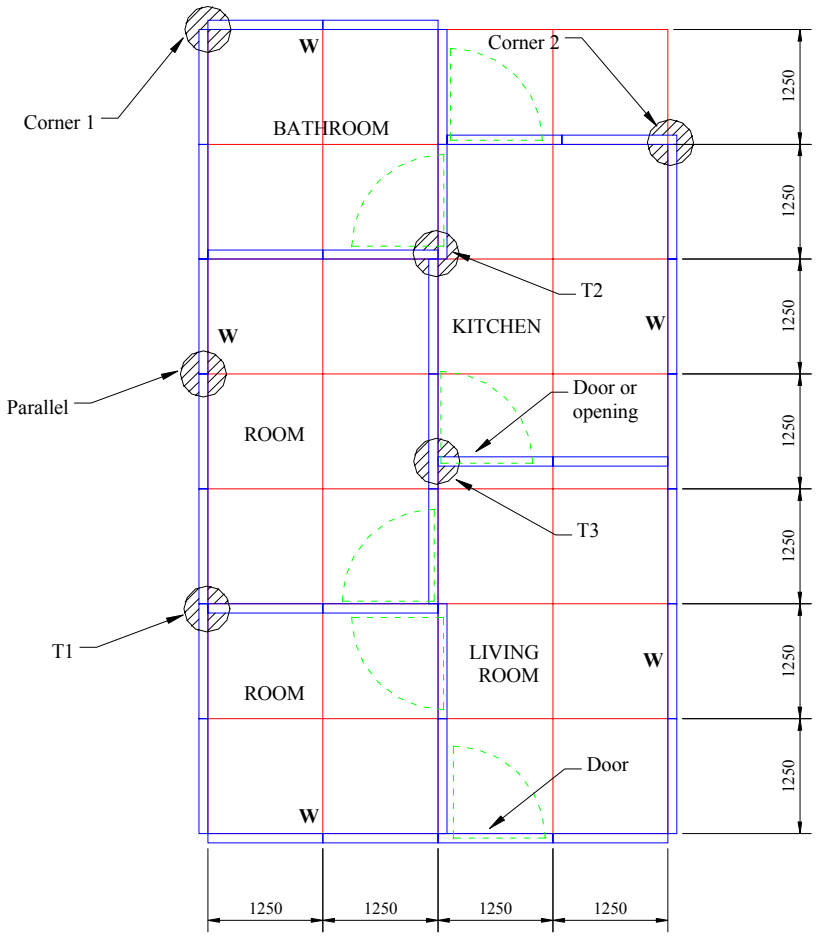

Figure B-1 Floor plan of house design example using prefabricated panels.

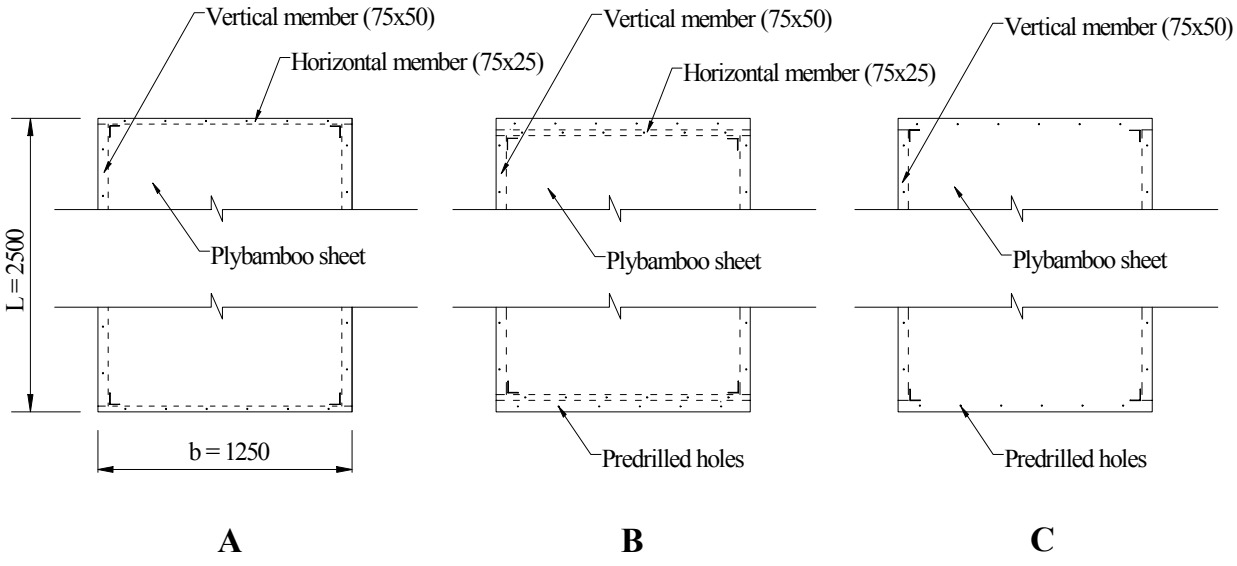

Figure B-2 Different possibilities for the prefabricated walls.

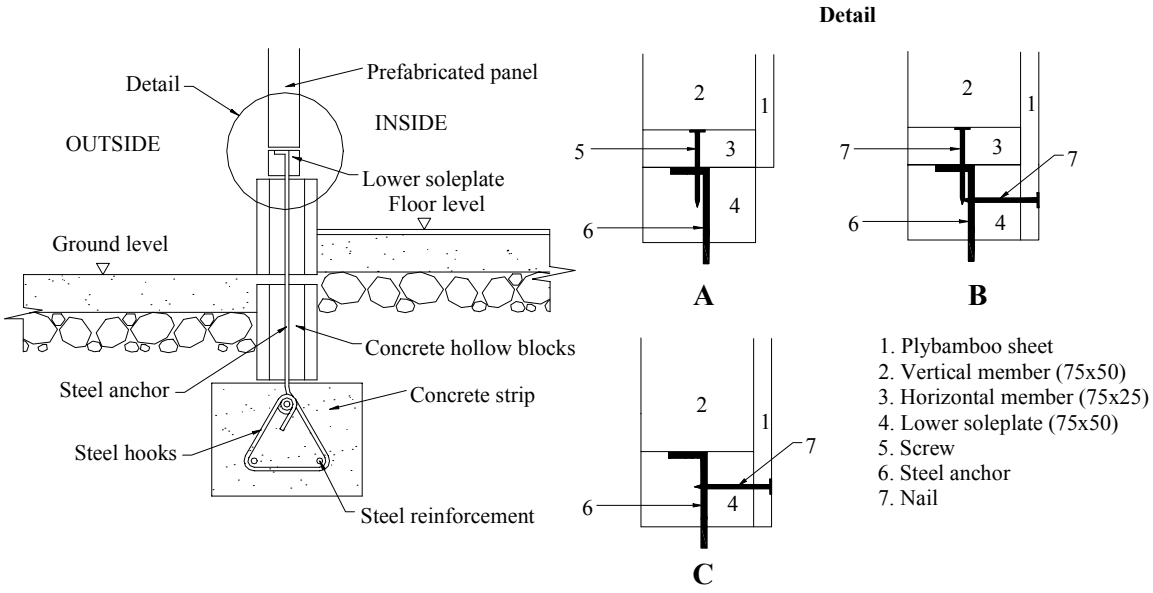

Figure B-3 Left: vertical section of the foundation. Right: Details of the wall to foundation connection depending on the type of panel.

The right part of Figure B-3 shows how each of the different types of panel would be connected to the lower soleplate. Note that for panel A, screws are needed to join the panel to the lower soleplate because these fasteners must prevent uplifting whereas in panel B, since the sheet is directly joined to the soleplate, nails would be sufficient to join the horizontal members to the lower soleplate.

B.4 Roof

The wall to roof connection will depend on the type of roof structure that is going to be used. Basically, this structure could be easily joined to the upper soleplate as shown in Figure B-4.

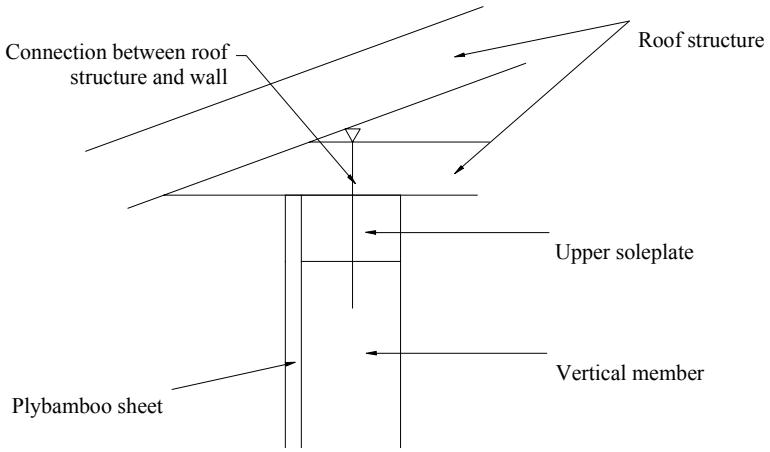

Figure B-4 Wall to roof connection for panel type C.

C. CALCULATION OF WIND AND SEISMIC LOADS

C.1 Calculation of wind load

The house design method must be able to withstand usual wind loads without deforming in certain range. Moreover, the house must be able to resist high wind loads caused by hurricanes without suffering collapse. Wind loads are very difficult to calculate accurately. Nevertheless, design codes give tools to calculate expected wind loads in a structure.
In the following example, the International Building Code 2000 (IBC 2000) [6] is adopted in order to calculate the wind loads acting on the house presented in appendix B.

Wind loads according to IBC 2000

Wind loads are based on Bernoulli's equation:

$$q = 0.5\rho v^2 \qquad \textbf{(C-1)}$$

Where, q is the wind pressure, ρ is the air density and v is the air velocity. In order to obtain the loads that are acting on certain structure, equation C-1 is modified by several factors such as shape, exposure, height and others. The wind speed is obtained from maps which indicate the maximum expected velocity in certain region.
Section 1609.6 gives simplified provisions to determine wind loads for low-rise buildings. The restrictions are given in section 1609.6.1.
Figure C-1 shows the maximum loads considered for the design example. These loads were obtained from tables 1609.6.2.1 (1) and 1609.6.2.1 (2) using a height and exposure coefficient of 1.21 from table 1609.6.2.1 (4). The importance factor I_w was taken from table 1604.5 as 1.00 whereas the load factor was taken as 1.6 (formula 16.6). The wind speed is 135 km/h (85 mph).

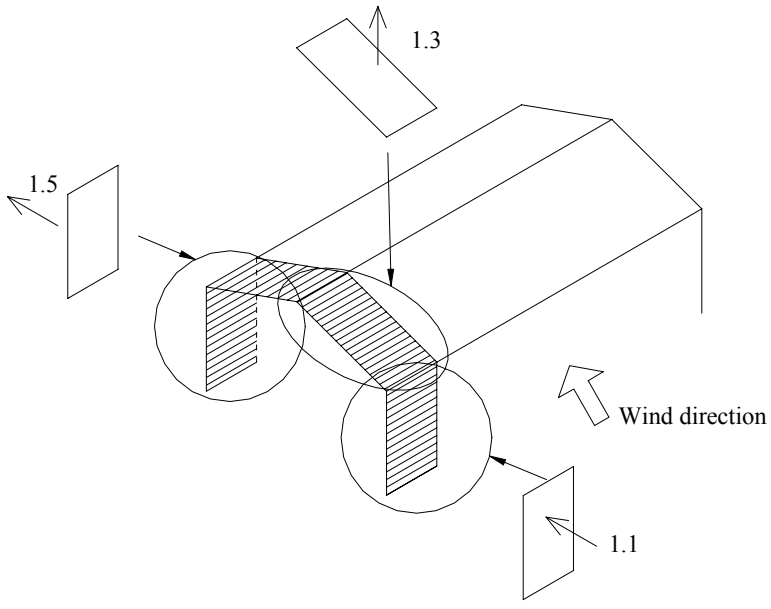

Figure C-1 Maximum wind loads (kN/m^2) considered for the design example.

C.2 Calculation of seismic loads

One of the advantages of the prefabricated plybamboo walls with respect to earthquakes is their lightness. The lighter the structure is the lesser the magnitude of the forces induced by the earthquake. As wind loads, seismic loads are difficult to calculate accurately and hence, design codes provide tools to calculate expected seismic forces in case of earthquake.

Seismic loads according to IBC 2000

Seismic loads are based on second Newton's motion law:

$$F = ma \qquad \textbf{(C-2)}$$

Where F is the load applied to the object, m is the object's mass and a is the object's acceleration. That is why, the formulas used in the codes have the following form:

$$F = CW \qquad \textbf{(C-3)}$$

Where F is the load applied to the structure, C is a coefficient (depending on several factors such as expected acceleration, type of soil, type of structure, fundamental period of the structure and others) and W is the weight of the structure.
For a one-story building such as a house, a simplified analysis procedure can be carried out. This analysis is described in section 1617.5. The seismic base shear, V, can be calculated with the following equation:

$$V = \frac{1.2 S_{DS}}{R} W \quad \text{(Equation 16-49 of reference 6)}$$

- Calculation of S_{DS}

  Combining equations 16-16 and 16-18, the following formula is obtained:

  $$S_{DS} = \frac{2}{3} F_a S_s \quad \text{(Equation 16-16 and 16-18)}$$

  Where, F_a is the value of site coefficient depending on the site class, S_s is the mapped spectral acceleration for short periods and S_{DS} is the design elastic response acceleration at short period.
  Assuming S_s = 1.0 (the maximum value in U.S.A is 2.0) and F_a = 1.1 [maximum value for S_s = 1.0 in table 1615.1.2 (1)] a value of S_{DS} = 0.73 is obtained.

- Calculation of R

  The response modification factor R is obtained from table 1617.6. For bearing wall systems composed by light frame walls with shear panels a value of R = 2.0 can be used.

- Calculation of W

  The total weight of the house will be given by the weight of the walls and the roof. The weight of one panel is the sum of the sheet (790x2.5x1.25x.012 = 30 kg), the vertical members (2x490x2.45x0.075x0.05 = 9 kg) and the horizontal members (2x490x1.25x0.075x0.05 = 4.6 kg) which gives a total of 43.6 kg per panel. Considering a wooden roof structure weighing 10 kg/m^2 and a light roof finish such as galvanized steel of 5 kg/m^2 a total roof weight of 15 kg/m^2 is obtained. For the house example showed in appendix A, the total house weight would be 34x43.6 + 15x44 = 2140 kg or 21.4 kN where 34 is the number of panels and 44 is the house area in m^2.

Introducing the calculated values in equation 16-49 of IBC 2000, the seismic base shear can be calculated as:

$$V = \frac{1.2x0.73}{2} W = 0.44W = 0.44x21.4 = 9.4\,\text{kN}.$$

There are at least three walls in one direction which means that each shear wall should carry a load of 9.4/3 = 3.1 kN.

D. CALCULATION OF JOINT CAPACITIES FOR NAILED AND SCREWED CONNECTIONS

The following calculations correspond to shear, withdrawal and moment capacities of each of the joints present in the corner connection and other connections of interest. In most cases they are neither design nor characteristic values but mean values. The purpose is to compare these values with experimental results. Hence, the equations used are calculated using the mean values (when a mean value is desired) instead of the design values.
The terms B1, B2, B3 and B4 are defined in section 3.5.
The number of the equations indicated in brackets corresponds to the number used in Eurocode 5 [7].

D.1 Nailed connections

D.1.1 Shear capacity in B2 and B3

From Figure D-1a and based on figure 6.2.1 of Eurocode 5 [7]:

$t_1 = 50\,\text{mm}.$
$t_2 = 38\,\text{mm}.$
$f_{h,1} = 0.082(1-0.01d)\rho = 0.082(1-0.01x4.1)490 = 38.5\,\text{N/mm}^2$ (Equation 6.3.1.2b).
$f_{h,2} = 0.082\rho d^{-0.3} = 0.082x490x4.1^{-0.3} = 26.3\,\text{N/mm}^2$ (Equation 6.3.1.2a).
$d = 4.1\,\text{mm}.$
$M_y = 180d^{2.6} = 180x4.1^{2.6} = 7055\,\text{Nmm}$ (Equation 6.3.1.2c).

With these parameters, it can be found that the shear capacity is 1479 N per nail (Equation 6.2.1f gives the lower value from the equations given in section 6.2.1 (1) [7]). The failure mode can be seen in Figure D-1b.

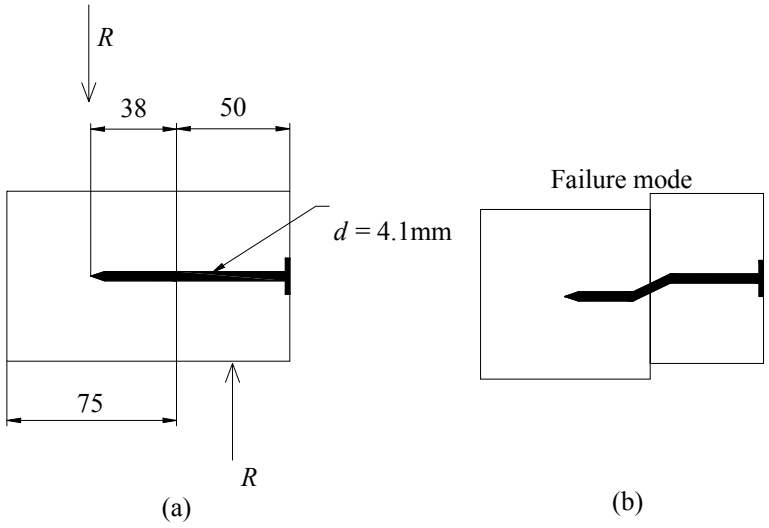

Figure D-1 (a) Parameters needed to calculate the shear capacity R. (b) Failure mode in shear for joint B2.

D.1.2 Withdrawal capacity in B2 and B3

From Figure D-1 and based on figure 6.3.2a of Eurocode 5 [7]:

$l = 38$ mm.
$d = 4.1$ mm.
$h = 50$ mm.
$f_1 = 18x10^{-6}\rho^2 = 18x10^{-6}x490^2 = 4.32$ N/mm^2 (Equation 6.3.2d).
$f_2 = 300x10^{-6}\rho = 300x10^{-6}x490^2 = 72.0$ N/mm^2 (Equation 6.3.2e).

With these parameters it can be found that the withdrawal capacity is 673 N per nail (Equation 6.3.2a). The failure corresponds to withdrawal of the nail in the member receiving the point.

D.1.3 Moment capacity in B2 and B3

The bending moment that B2 could transmit would be given by a tensional force in the nail and a compression force produced by the contact between the two pieces of wood (see Figure D-2).

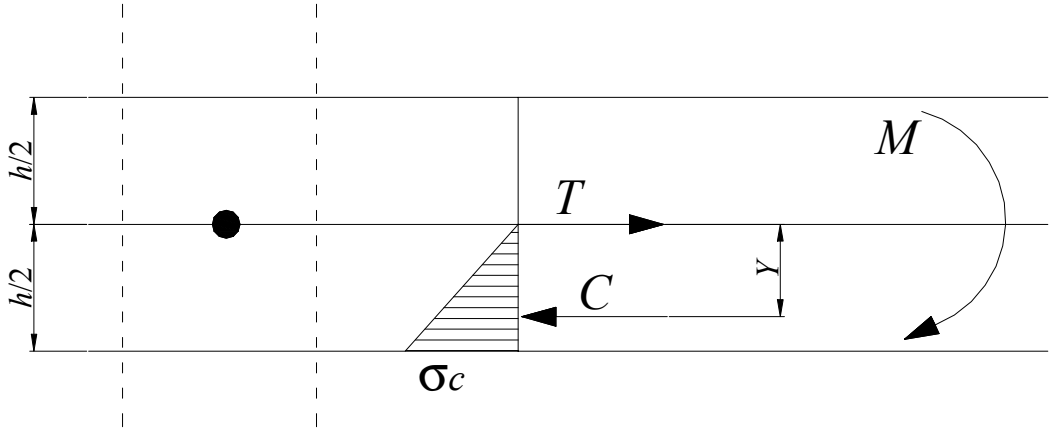

Figure D-2 Bending moment transmitted by B2.

From Figure D-2, the following equations can be derived:

$$T = C \quad \textbf{(D-1)}$$

$$M = CY = TY \quad \textbf{(D-2)}$$

The maximum moment would be produced when the only contact point between the pieces is at the very bottom. In this case $Y = h/2$. Hence, for $h = 75$ mm,

$$M_{max} = 37.5T \quad \textbf{(D-3)}$$

The maximum tensional force would correspond to the withdrawal capacity of the nail calculated on the previous section as 673 N. That means that the maximum bending moment that B2 can transmit is 37.5x673 = 25237 Nmm per nail. The yielding moment would be approximately two thirds of the maximum moment if the compression stresses vary linearly.

D.1.4 Shear capacity in B1 and B4

From Figure D-3a and based on figure 6.2.1 of Eurocode 5 [7]:

$t_1 = 12$ mm.
$t_2 = 43$ mm.
$f_{h,1} = 92.5$ N/mm^2 [2].
$f_{h,2} = 0.082\rho d^{-0.3} = 0.082x490x2.8^{-0.3} = 29.5$ N/mm^2 (Equation 6.3.1.2a).
$d = 2.8$ mm.
$M_y = 180d^{2.6} = 180x2.8^{2.6} = 2617$ Nmm (Equation 6.3.1.2c).

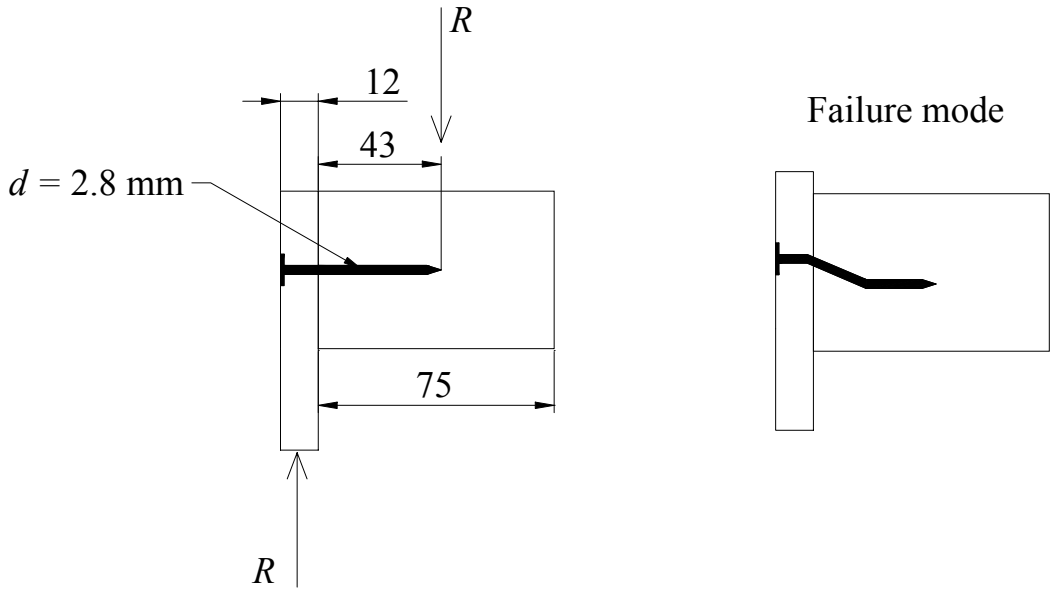

Figure D-3 (a) Parameters needed to calculate the shear capacity R. (b) Failure mode in shear for joint B4.

With these parameters, it can be found that the shear capacity is 891 N per nail (Equation 6.2.1f). The failure mode can be seen in Figure D-3b.

D.1.5 Withdrawal capacity in B1 and B4

From Figure D-3a (and based on figure 6.3.2a of Eurocode 5):

$l = 43$ mm.
$d = 2.8$ mm.
$h = 12$ mm.
$f_1 = 18x10^{-6}\rho^2 = 18x10^{-6}x490^2 = 4.32$ N/mm^2 (Equation 6.3.2d).
$f_2 = 300x10^{-6}\rho = 300x10^{-6}x790^2 = 187$ N/mm^2 (Equation 6.3.2e).

With these parameters it can be found that the withdrawal capacity is 520 N per nail (Equation 6.3.2a). The failure corresponds to withdrawal of the nail in the member receiving the point.

D.1.6 Moment capacity in B1 and B4

The same approach for the moment in B2 (D.1.3) is adopted. In this case h = 50 mm and:

$$M_{max} = 25T \qquad \textbf{(D-4)}$$

The maximum tensional force would correspond to the withdrawal capacity of the nail calculated on the previous section as 520 N. That means that the maximum bending moment that B4 can transmit is 25x520 = 13000 Nmm per nail.

D.2 Screwed connections

In case that screwed connections are used to join the plybamboo sheets to the vertical elements the joint capacities in B1 and B4 could increase considerably. Especially the withdrawal resistance and consequently the moment capacity.

D.2.1 Shear capacity in B1 and B4

According to Eurocode 5 (6.7.1) for screws with a diameter less than 8 mm, the rules for nails apply. The used screw has a diameter of 4.9 mm and is 49 mm long. The root diameter (the threaded part is not taken into account) is about 3 mm. The effective length is 46 mm (the head is not taken into account).

The parameters would be as follows:

$t_1 = 12$ mm.
$t_2 = 34$ mm. ($46 - 12$)
$f_{h,1} = 92.5$ N/mm^2 [2].
$f_{h,2} = 0.082(1 - 0.01d)\rho = 0.082(1 - 0.01x4.9)490 = 38.2$ N/mm^2 (Equation 6.3.1.2b).
$d = 4.9$ mm.
$M_y = 180d^{2.6} = 180x3.9^{2.6} = 6195$ Nmm (Equation 6.3.1.2c). 80 % of the diameter is used.

Eurocode 5 recommends 90% when the root diameter is at least 70% of the shank diameter. In this case the root diameter is just 60% and that is why the 80% was used.

With these parameters, it can be found that the shear capacity is 1990 N per screw (Equation 6.2.1f). The failure mode can be seen in Figure D-3b.

D.2.2 Withdrawal capacity in B1 and B4

The parameters needed to obtain the withdrawal capacity of a screw according to Eurocode 5 are:

$f_3 = (1.5 + 0.6d)\sqrt{\rho} = (1.5 + 0.6x4.9)\sqrt{490} = 98.3$ N/mm (Equation 6.7.2b)
$l_{ef} = 34$ mm ($46 - 12$) which is the length of the threaded part in the member receiving the point.

With these parameters it can be found that the withdrawal capacity is 2860 N per nail (Equation 6.7.2a). The failure corresponds to withdrawal of the nail in the member receiving the point.

D.3.3 Moment capacity in B4

With equation D4 and the withdrawal capacity obtained in the previous section a moment capacity of 71500 Nmm is obtained.

E. EXPERIMENTAL CURVES FOR SHEET TO FRAME CONNECTION UNDER LATERAL LOAD

Figure E-1 shows all the curves obtained from each of the tests that were made in order to obtained the lateral capacity of the sheet to frame connection (see chapter 5).

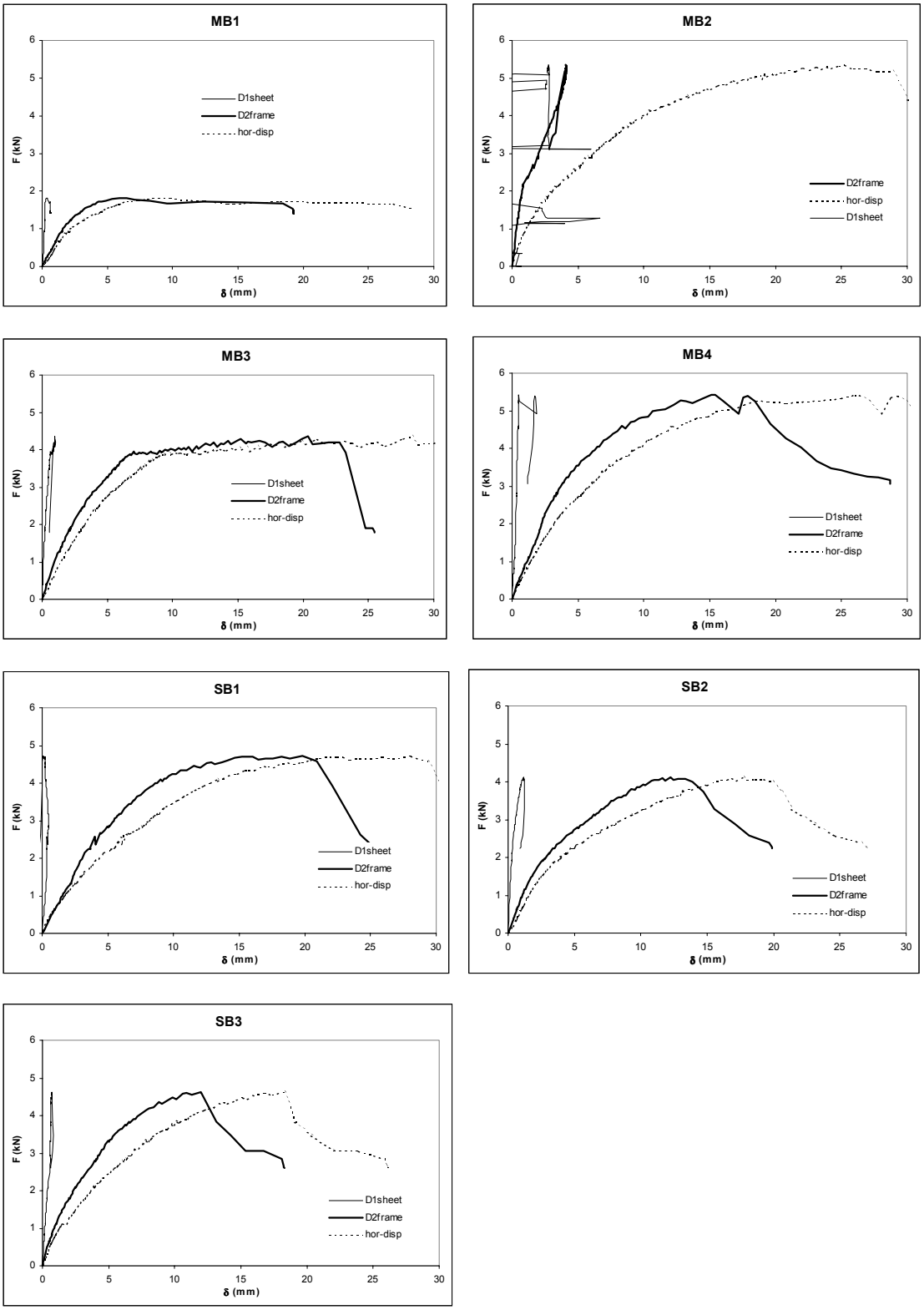

Figure E-1 Load-deflection curves for each of the tests for sheet to frame connection under lateral load.

F. CALCULATION OF DESIGN VALUES OF SEVERAL JOINTS AND MEMBERS

The following are calculations based on Eurocode 5 [7] and Table A-1. The results are considered for some structural calculations made on chapter 2.

F.1 Top and bottom connection

Figure F-1 shows a steel-to-wood joint for a thin steel plate ($t \leq 0.5d$, see section 6.2.2 of reference 7). In this case t = 2 mm and d = 4 mm. According to Eurocode 5 [7], the shear capacity R of this joint is calculated with one of the following equations:

$R = 0.4 f_{h,1,d} t_1 d$ (Equation 6.2.2a) or,

$R = 1.1\sqrt{2 M_{y,d} f_{h,1,d} d}$ (Equation 6.2.2b).

The minimum value of the previous two equations is used for design. Hence, the shear capacity of the joint between the vertical members and the soleplates (section 2.4) is obtained as follows:

$f_{h,1,k} = 0.082(1-0.01d)\rho_k = 0.082(1-0.01x4)350 = 27.6\,\text{N/mm}^2$ (Equation 6.3.1.2b).

The value ρ_k = 350 kg/m^3 is taken from reference 4, table 1, page A7/3 for wood class C24.

$f_{h,1,d} = f_{h,1,k} k_{\text{mod}} / \gamma_M = 27.6x1.1/1.3 = 23.4\,\text{N/mm}^2$ (Equation 2.2.3.2a).

$t_1 = 30$ mm (35-5 taken into account the thickness of the steel plate and the head of the screw).

$d = 4$ mm

$M_{y,k} = 180 d^{2.6} = 180x3.2^{2.6} = 3704\,\text{Nmm}$ (Equation 6.3.1.2c). The diameter is taken as 80% as explained in section D.2.1).

$M_{y,d} = 3704x1.1/1.3 = 3367\,\text{Nmm}$ (Equation 2.2.3.2a).

$R = 0.4x23.4x30x4 = 1123$ N (Equation 6.2.2a) or,

$R = 1.1\sqrt{2x3367x23.4x4} = 873\,\text{N}$ (Equation 6.2.2b).

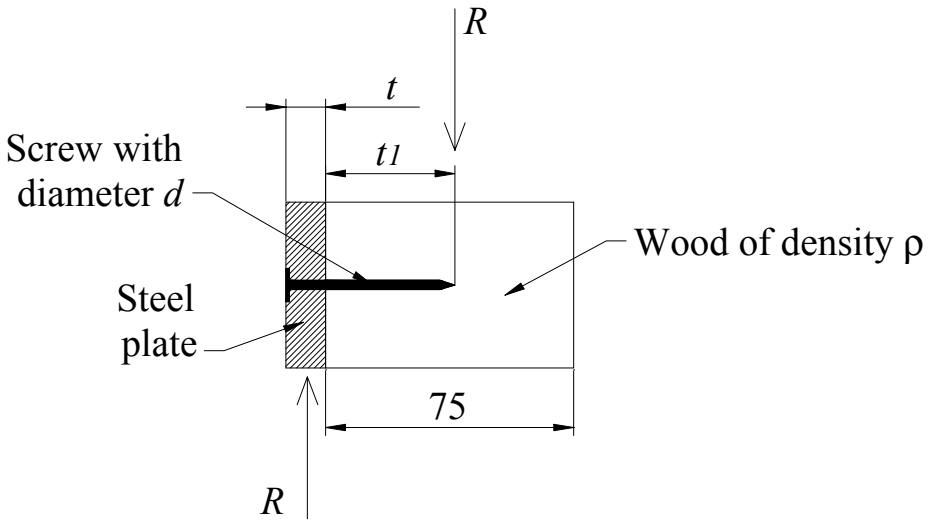

Figure F-1 Parameters needed in order to calculate the shear capacity R on the steel-to-timber connection.

Hence, the joint shear capacity is R = 873 N per screw.

F.2 Shear capacity in a plybamboo-to-wood joint

Following the same approach of section D.1.4 but using design values instead of mean values the joint capacity is calculated.

$t_1 = 12$ mm.
$t_2 = 43$ mm.
$f_{h,1,d} = 68$ N/mm^2 [2].
$f_{h,2,k} = 0.082\rho d^{-0.3} = 0.082x350x2.8^{-0.3} = 21.1$ N/mm^2 (Equation 6.3.1.2a).
$f_{h,2,d} = 21.1x1.1/1.3 = 17.8$ N/mm^2.
$d = 2.8$ mm.
$M_y = 180d^{2.6} = 180x2.8^{2.6} = 2617$ Nmm (Equation 6.3.1.2c).
$M_{y,d} = 2617/1.1 = 2379$ Nmm.

With these parameters, it can be found that the shear capacity is 675 N per nail (Equation 6.2.1f). The failure mode can be seen in Figure D-3b.

F.3 Withdrawal capacity of screws in timber-to-timber joints

The connection between the lower horizontal member and lower soleplate in panel type A (Figure B-2) must be screwed. The capacity of this connection to avoid uplifting will depend on the withdrawal capacity of the screws. Following the same approach of section D.2.2 but using design values instead of mean values the joint capacity is calculated. Hence,

$f_{3,k} = (1.5 + 0.6d)\sqrt{\rho} = (1.5 + 0.6x4.9)\sqrt{350} = 83.1\,\text{N/mm}.$

$f_{3,d} = 83.1x1.1/1.3 = 70.3\,\text{N/mm}^2.$

$l_{ef} = 21\,\text{mm}\ (46 - 25)$ which is the length of the threaded part in the member receiving the point.

With these parameters it can be found that the withdrawal capacity is 1130 N per screw (Equation 6.7.2a). The failure corresponds to withdrawal of the screw in the member receiving the point.

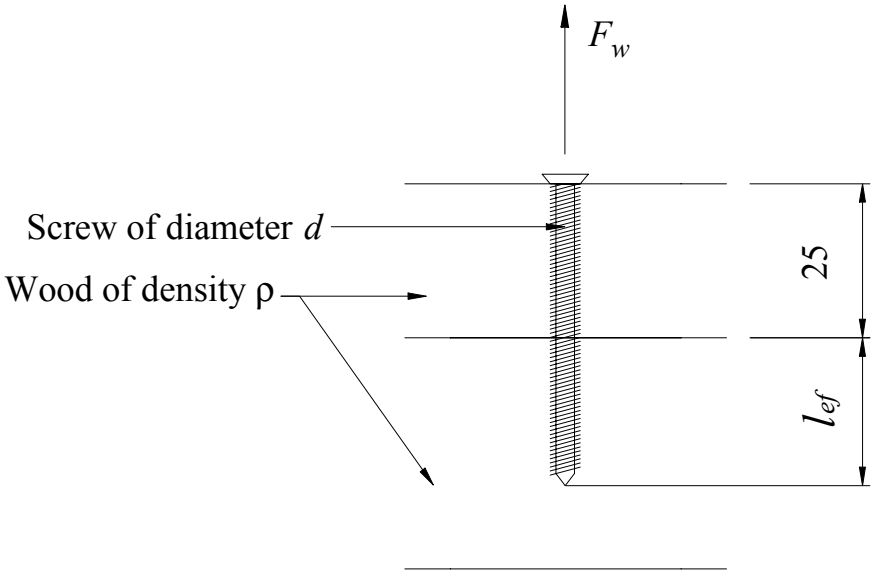

Figure F-2 Parameters needed to calculate the withdrawal capacity of the joint.

In the case of suction, where the plybamboo sheets are held by screws, the effective length would be 46-12 (sheet thickness) = 34 mm. Repeating the previous procedure, a withdrawal capacity of 2040 N per screw is found.

F.4 Design buckling resistance of vertical members

The buckling resistance of the vertical members is calculated according to Eurocode 5 [7]. The number of the equations indicated in brackets corresponds to the number used in Eurocode 5 [7].

$\sigma_{c,crit} = \frac{\pi^2 E_{0.05}}{\lambda^2}$ (5.2.1c or 5.2.1d).

$E_{0.05}$ = 7400 N/mm^2 (reference 4, table 1, page A7/3 for wood class C24).

$\lambda^2 = \frac{AL_{ef}}{I} = \frac{hbL_{ef}}{hb^3/12} = \frac{75x50x2400}{75x50^3/12} = 27648\ \text{mm}^{-1}$. (since the cross-section of the member is rectangular, the lower I is taken into account). Hence,

$\sigma_{c,crit} = \frac{\pi^2 x7400}{27648^2} = 2.64\ \text{N/mm}^2$.

$\lambda_{rel} = \sqrt{\frac{f_{c,o,k}}{\sigma_{c,crit}}} = \sqrt{\frac{21}{2.64}} = 2.82$ (5.2.1a or 5.2.1b), $f_{c,o,k}$ is taken from reference 4, table 1, page A7/3 for wood class C24.

$k = 0.5\left(1 + \beta_c\left(\lambda_{rel} - 0.5\right) + {\lambda_{rel}}^2\right) = 0.5\left(1 + 0.2\left(2.82 - 0.5\right) + 2.82^2\right) = 4.71$ (5.2.1h), β_c is 0.2 for solid timber.

$k_c = \frac{1}{k + \sqrt{k^2 - {\lambda_{rel}}^2}} = \frac{1}{4.71 + \sqrt{4.71^2 - 2.82^2}} = 0.118$ (5.2.1g).

Finally, $\sigma_{c,o,d} \le k_c f_{c,o,d} \Rightarrow \sigma_{c,o,d} \le 0.118x17.8 = 2.1\ \text{N/mm}^2$ (5.2.1e or 5.2.1f),

$f_{c,o,d} = f_{c,o,k} k_{\text{mod}} / \gamma_M = 21x1.1/1.3 = 17.8\ \text{N/mm}^2$.

The design buckling resistance of the vertical member is,

$P_{cr,d} = \sigma_{c,o,d} A = 2.1x75x50 = 7875\ \text{N}$.